Electronic Thesis and Dissertation Repository

11-16-2017 5:00 PM

Binding of Salivary Proteins to Orthodontic Brackets

Maria Pia Canales, *The University of Western Ontario*

Supervisor: Siqueira, Walter, *The University of Western Ontario*
A thesis submitted in partial fulfillment of the requirements for the Master of Clinical Science degree in Orthodontics
© Maria Pia Canales 2017

Follow this and additional works at: https://ir.lib.uwo.ca/etd

⚙ Part of the Dental Materials Commons, and the Orthodontics and Orthodontology Commons

Binding of Salivary Proteins to Orthodontic Brackets

ABSTRACT:

Objectives: The aim of this study was to investigate the effect of different orthodontic materials on the formation of the protein pellicle on the bracket surface.

Materials and Methods: We used X-ray Photoelectron Spectroscopy (XPS) to analyze the atomic composition of orthodontic metallic and ceramic brackets. Following XPS, the brackets were immersed in human whole saliva supernatant for 2-hour incubation at 37°C. Hydroxyapatite (HA) discs were used as control. Acquired pellicle was harvested with sonication for each group, and liquid chromatography electrospray ionisation mass spectrometry was used for protein identification.

Results: Differences reported by XPS and mass spectrometry were noted among the tested groups. Most of the proteins present on the acquired pellicle were identified specifically to each group, indicating little overlap in the acquired pellicle proteins; 84% of proteins present on the HA discs were unique to this group, 74% were unique to ceramic brackets and 79% were unique to metallic brackets. Despite the fact that most proteins were unique to each bracket material, proteins related to antimicrobial, lubrication and remineralization biological functions were present in all groups. However, proteins associated with inflammatory processes and biofilm formation were found only on ceramic brackets.

Conclusions: The results demonstrate that the protein pellicle formed on the bracket surface is dependent on the molecular composition of the bracket. Therefore, our findings suggest that modulation of the bracket pellicle via alteration of bracket surface is a possibility.

Key words: orthodontic brackets, acquired enamel pellicle (AEP), Acquired bracket pellicle (ABP), X-ray Photoelectron Spectroscopy (XPS), Mass Spectrometry, LC-ESI-MS/MS, Protein Identification, Dental caries, white spot lesions (WSL)

Co-Authorship:

The completion of this thesis was possible due to the contribution of several individuals. It would not have been possible without their valued time and efforts, which was greatly appreciated.

Maria Pia Canales:	DMD, Master of Clinical Dentistry Candidate, Graduate Orthodontics
Contribution:	Manipulation of all laboratory experiment, data collection and analysis of all experiments, author manuscript
Walter Siqueira:	DDS, PhD Thesis supervisor Associate Professor, Dentistry Associate Professor, Biochemistry
Contribution:	Study design, data analysis for XPS and mass spectrometry, reviewed manuscript
Karla Crosara:	DDS
Contribution: mass	Study design, data collection and analysis for XPS and spectrometry, reviewed manuscript
Camila Martins:	DDS
Contribution:	Manipulation of all laboratory experiment, data collection and analysis of all experiments and reviewed manuscript

Acknowledgement:

I would like to express my sincere gratitude to all colleagues, friends and teachers that have contributed to the accomplishment of this project.

I would first like to thank my supervisor, Dr. Walter Siqueira, for taking on an amateur research student like myself. Your guidance and patience from day one have been invaluable in allowing me to progress through this project. Thank you for your time, knowledge, effort and especially your passion throughout this journey.

I am very grateful that I have been helped by Karla Crosara since the beginning of this project. You have been a key player in the smooth progression of this thesis and I have truly enjoyed working with you. Thank you for all your knowledge, expertise, tips and patience. I could not have asked for a better research co-supervisor. Good luck on your PhD degree.

Thank you to my friend and colleague Camila Martins; your hard work in every step of this project was greatly appreciated. You were always prepared to help me and made this project enjoyable. I certainly had a great time with you in the lab!

A special thanks to Siqueira Lab members who were always ready to help me with laboratory techniques. I would also like to thank the saliva donors who contributed to this project; thank you for your contributions.

Thank you to my friend Dr. Jonathan Albilia for your many corrections on my franco-spanish misspelled words. Thank you for your time and patience.

I would also like to thank American Orthodontics for their generous contribution, allowing

Table of Contents

List of Tables

List of Figures

List of Abbreviations

ABP	Acquired Bracket Pellicle
AEP	Acquired enamel pellicle
BCA	Bicinchonic acid
BE	Binding energy
BMQ	metallic orthodontic brackets
CBMQ	Ceramic orthodontic brackets
DMQ	Disc MiliQ water
HA	Hydroxyapatite
IgA	Immunoglobulin A
IgG	Immunoglobulin G
IgM	Immunoglobulin M
LC-ESI-MS/MS	Liquid chromatography-electrospray ionization-tandem mass spectrometry
MUC5B	High molecular weight mucin glycoprotein
MUC7	Low molecular weight mucin glycoprotein
MIM	Metal injection molding
SF	Salivary flow
SS	Stainless Steel
WSS	Whole saliva supernatant
XPS	X-ray photoelectron spectroscopy

CHAPTER 1: Orthodontic and Pellicle

1.1 Introduction

A constant concern in the orthodontic clinic is the high prevalence of active carious lesions in patients undergoing treatment. In fact, it has been noted that 30 to 70% of patients experience active caries lesions during orthodontic treatment (1,2). A Previous study (3) described an alarming increase of 2.5 times in active non-cavited carious lesions in orthodontic patients compared with the normal population. It is also reported that orthodontic appliances decrease the saliva's buffering capacity and decrease the quantity of salivary α-amylase after they are in place for 3 and 6 months, suggesting that the properties of saliva of orthodontic patients are subject to changes (3). This may have a repercussion on the rate of active caries lesions, as the severity of these lesions can progress from active white spots to frank cavitation of the enamel.

It is well known that the level of bacterial growth on the surface of the orthodontic brackets is variable depending on the material of the bracket (4-6). Furthermore, composite brackets have been reported to attract bacterial colonization at a rate higher than any other bracket (7). Several studies have focused on the initial bacterial binding to different orthodontic brackets (5,8,9) trying to understand which material is more prone to cariogenic bacterial adhesion. However, there is little information in the literature about the protein pellicle that initially adheres to the brackets.

In the oral cavity, it is recognized that specific proteins/peptides have a greater affinity for enamel than others, based in part on their surface charges (10). The acquired enamel pellicle (AEP) is a thin protein layer formed on the tooth surface that plays a key role in the maintenance of oral health by regulating processes such as lubrication, demineralization, and remineralization (11). The AEP

also influences the composition of the early microbial flora adhering to tooth surfaces (11). Nevertheless, salivary pellicles are not limited to the surface of the tooth. These are also present on the oral mucosa (12), dental appliances like orthodontic brackets (8), and even restorations and titanium implants (13).

In a previous investigation (14), Liquid Chromatography – ElectroSpray Ionization tandem Mass Spectrometry (LC-ESI-MS/MS) was used to investigate the protein composition of the *in vivo* AEP. This study disclosed that this natural film contains at least 130 different proteins. Through proteomic analysis, it is possible to discover the salivary components of the AEP. It will be interesting to use this advanced technology to understand protein pellicles specific to orthodontic brackets, which will provide an awareness and understanding of the future biofilm formation.

The mechanism by which proteins adhere to surfaces is heavily determined by physico-chemical properties of the material. Therefore, analyzing the nanostructure of orthodontic brackets, for example, may provide important information regarding the reasons why specific proteins may selectively adhere to orthodontic fixed appliances. X-ray photoelectron spectrometry (XPS) is a powerful tool that gives information about elemental distributions, coating structure and surface functionality of materials (15). XPS can detect all elements (except hydrogen and helium) (10) and can provide information on particle sizes in the 1-20 nm scale (15). XPS probes the surface of the sample to a depth of 5-10 nanometers (10) and provides a complete profile about the composition of a sample near the surface area, which is the region directly in contact with the oral cavity.

Since orthodontic treatment lasts for an average of two years, the composition of the protein pellicle on the bracket surface, and the consequent biofilm formation, will have a selective impact on the abundance of specific oral microorganisms.

The objectives of this study were:

1. to investigate the molecular composition of two types of orthodontic brackets (metallic and ceramic);

2. to characterize the composition of the acquired protein pellicle formed on the surface of the different orthodontic brackets; and

3. to investigate the correlation between the molecular composition of the bracket surface and the proteins identified in the acquired bracket pellicle.

Our findings will attempt to give more information on the uncharacterized acquired bracket pellicle for a future possible way to modulate it to reduce oral biofilm formation on the surface of orthodontic brackets.

1.2 Literature Review:

1.2.1 Orthodontic treatment and Dental Caries:

White spot lesions are the precursor of dental cavitation and they are a constant concern for clinicians and orthodontic patients. A white spot lesion is the first clinical sign of active dental caries, and thus allow for early diagnosis (3). Organic acids produced mainly by cariogenic streptococci can be responsible for this demineralization (16). Furthermore, tooth demineralization has been reported to be the most common complication of fixed orthodontic treatment, present in 50% of orthodontic patients (17). In only four weeks, this unaesthetic lesion can appear on the surface of the enamel (18). Orthodontic patients are very prone to develop these lesions because of the difficulty in maintaining excellent oral hygiene. Most orthodontic patients also wear orthodontic adjuvant devices (ex: power chains, open coils, closed coils) that can cause a significant increase in plaque retention, possibly compromising their oral health. In addition, it has been suggested that metallic orthodontic brackets decrease the salivary pH (19) and increase colonization by Streptococcus mutans (20).

Several studies have focused on the initial bacterial binding to different orthodontic brackets (5,8,9) trying to understand which material is more prone to cariogenic bacterial adhesion. Effectively, the composition of the initial bacterial attachment differs depending on the surface material of the bracket (6,21). It has been reported that qualitative and quantitative variations were observed on the biofilm after only 30 to 60 mins of intra-oral exposure of different brackets (21). Furthermore, it also has been demonstrated that the affinity for Streptococcus mutans is significantly lower on metallic brackets compared with the other materials (22). However, little

information is available on the adhesion of various proteins to different orthodontic brackets, which may impact biofilm formation.

1.2.2 <u>Saliva characteristics:</u>

1.2.2.1 *<u>Saliva definition and composition:</u>*

Saliva is a clear, slightly acidic (pH 6 to 7) and mucoserous exocrine secretion. It contains 99% water, electrolytes (sodium, potassium, calcium, chloride, magnesium, bicarbonate, phosphate), immunoglobulins, mucins and other proteins. Glucose and nitrogenous products (urea and ammonia) are also present in the saliva (23,24).

1.2.2.2 *<u>Whole saliva:</u>*

Whole saliva (or total) is a complex fluid mixture derived from major and minor salivary glands, crevicular fluid, oral mucosa transudate, mucous of the nasal cavity and pharynx, non-adherent oral bacteria, food remainders, desquamated epithelial cells and blood cells. Traces of medications or chemical products found in the systemic circulation can also be detected (23). Whole saliva include stimulated and unstimulated saliva.

There are different methods available for collecting whole saliva. Common methods include spitting, suction, and swab (absorbent), Fejerskov & Kidd (25) reported that salivary composition varies according to the nature of the stimulus (gustatory or mechanical) and on the duration. A study of unstimulated, chewing-stimulated, and pure parotid saliva has revealed differences in metabolite profiles between the three types of saliva (26). These results reinforce the importance

of using the same saliva collection method when comparing protein levels within a study or among studies.

1.2.2.3 _Salivary glands:_

The major salivary glands include paired parotid, submandibular and sublingual glands. Thousands of proteins could be identified in the major salivary glands compare to only 56 proteins in the minor salivary glands (27). Minor glands are multiple small glands found around the entire oral cavity, except for the gingivae, anterior hard palate and tongue dorsum (28). They contribute 10% of the total volume of human saliva (29). They have been reported to have a relative enrichment of mucins (MUC5B and MUC7) and immunoglobulins (8 different types) (27). Siqueira reported that there is a unique protein composition from minor salivary gland saliva (27). Cystatins, large salivary-proline-rich protein family, histatins and 12 new salivary proteins have been noted (27).

1.2.2.4 _Salivary flow:_

At rest, there is a small and continuous salivary flow of 0.3-0.5 mL/min (28). During that unstimulated state, the percentage contributions of the salivary glands are 20% from the parotids and 65% from submandibular (24). Furthermore, the unstimulated flow rate from all the minor salivary glands in the mouth has been reported to 7–8% of the unstimulated flow rate of whole saliva (29).

Stimulated saliva is produced by a mechanical, gustatory, olfactory or pharmacological stimulus. It represents 80-90% of daily salivary production (23). The percentage contribution of the parotid salivary glands drastically change to more than 50% when saliva is stimulated (30).

The saliva rate and the concentration level of salivary components vary according to the time of the day (31). Circadian low flow occurs during sleep, and peaks during stimulation periods (24). The unstimulated flow rate for parotid, submandibular and whole saliva attain a peak value around 15h30 and fall virtually to zero during sleep (32). This has a big implication in preventive dentistry. The age of the subject can also be a factor on protein concentration of the unstimulated saliva (33). For stimulated saliva, protein concentration can change depending on the flow rate, the nature of the stimulus, the duration of the stimulation, the circadian rhythm and the effects of previous exercise (32,34,35).

The saliva is first formed inside the acini; this saliva is isotonic with respect to plasma. It becomes hypotonic after it runs through the network of ducts (36). There is a low level of glucose, sodium, chloride and urea in the hypotonic saliva that allows the dissolution of substances and allows the gustatory buds to perceive different flavors. One important protein for the growth and maturation of the gustatory buds is gustatin (24).

Both sympathetic and parasympathetic nerve fibers innervate the salivary glands. When sympathetic innervation takes control, the salivary secretions contain more proteins (mucous). However, when the parasympathetic system dominates, the saliva will be more serous (30).

1.2.2.5 *Type of secretion:*

The saliva is first secreted in the acinar cells, these cells determine the type of secretion produced from the different salivary glands. There are three types of secretions: serous, mucous or mixed. The principal producer of serous secretions are the parotid glands and mucous secretions come

from the minor glands. Mixed secretions (mucous and serous) are in general produced by the sublingual and submandibular glands (24).

Parotid saliva contains amylase, proline-rich proteins and agglutinins. It also contains some amount of cystatins, lysozymes and extraparotid glycoproteins (24). Furthermore, parotid glands are by far the main source of amylase in whole saliva, but doesn't secrete mucins (34). In consequence, the percentage contribution of parotid to whole saliva will influence the relative proteins proportions. Sublingual saliva consists of a high concentration of both types of mucins (MUC5B and MUC7) and high levels of lysozymes (24). Furthermore, palatine secretions will have important concentration of MUC5B mucins and relatively high amylase concentrations (37).

1.2.2.6 *Role of saliva:*

Salivary function can be separated into 5 major groups for maintaining oral health and creating an appropriate ecologic balance. The five major roles are: (1) lubrication and protection, (2) buffering action and clearance, (3) maintenance of tooth integrity, (4) antibacterial activity, and (5) taste and digestion (38,39).

Lubrication and protection of the oral tissues against irritating agents is possible due to mucins (24). Macromolecules (proteins and mucins) will also serve to cleanse, aggregate and attach oral microorganism. This will have an impact on dental plaque metabolism (24).

The importance of buffering capacity of the saliva will prevent colonization by potential pathogenic microorganism. Effectively, bicarbonate, phosphates and urea will modulate the pH and the buffering capacity of saliva (24). Bicarbonate is the most important buffering system because it diffuses into plaque and neutralize acids (24). Furthermore, peptides rich in histidine

also are direct buffers after diffusion into the plaque (40). When salivary flow increases, the concentrations of total protein, sodium, calcium, chloride, bicarbonate and the pH will increase to different levels, but the concentration of inorganic phosphate and magnesium will decrease (24).

Enamel demineralization prevention by neutralizing the acids, coming from acidogenic microorganism, is possible due to calcium, phosphate, fluoride and proteins (11). The mechanisms by which AEP proteins (histatins, statherin and mucins) contribute to the enamel demineralization protection maybe be related on retarding enamel loss during acid challenges (11).

The antibacterial function comes from the immunoglobulins (IgA, IgG and IgM), proteins and enzymes (lactoferin, lysozymes and peroxidase) present in the saliva. IgA, however, is the largest immunologic component of saliva (24).

1.2.2.7 *Proteins:*

Salivary proteins are multifunctional, they can be functionally redundant, and they can act both for and against the host (41). Statherins, histatins, cystatins, and proline-rich proteins are proteins present in the protective pellicle, acquired enamel pellicle (AEP). They bind to hydroxyapatite and help control the crystalline growth of the enamel. They limit the dissolution of the minerals and allow the penetration of minerals into the enamel (24).

Proteins such as glycoproteins, statherins, agglutinins, histatins, and proline-rich proteins can aggregate bacteria to reduce their ability to adhere to hard/soft tissue surfaces. This in turn will control bacterial, fungal, and viral colonization (24).

Histatins:

Negative salivary proteins like histatin 1 have been reported to have a strong affinity to hydroxyapatite (HA) discs and they are considered pellicle precursors (10). Research has shown that histatins 1 have a buffering function, as well as strong antifungal and antibacterial activities (42). They can also modulate mineral formation and provide a protection against acid injury (43).

Statherin:

Statherin is a low molecular weight protein and is negatively charged. It can inhibit primary and secondary calcium phosphate precipitation (10). This will inevitably affect the control of dental calculus formation and remineralization of early dental caries (10). Statherin also facilitates the binding of Actinomyces viscous (45) and Fusobacterium nucleatum (46), determinant initial microbial colonizers of tooth surface.

Cystatins:

Human saliva contains multiple forms of cystatins; they all belong to family 2 of the cystatin superfamily (47). Some cystatins can have a neutral pI (cystatin SN) and others an acidic pI (cystatin SA) (47). Cystatins are considered as one of the most abundant proteins in the AEP on in situ studies (11). It demonstrates an affinity to mineral surfaces and can also inhibit calcium phosphate precipitation (48). Cystatins play an important role in maintaining the integrity of teeth (48).

Proline-Rich-Proteins (PRP) :

Proline-rich proteins are major components of parotid and submandibular human saliva. They can be divided into three groups; glycosylated, basic and acidic proline-rich proteins. The unique structure of the acidic proline-rich proteins doesn't belong to any known protein family. Furthermore, this protein has a role on the inhibition of hydroxyapatite formation. (49).

Mucins:

Mucins are proteins with a high carbohydrate content. MUC5B and MUC7 are the major members of the salivary mucin family (27). They are synthesized and secreted by submandibular, sublingual and minor salivary glands (50). In the oral cavity, they play an integral role in non-immune protection (51). They are responsible for lubrication, and protection against desiccation and environmental insult. They also have an important antimicrobial effect against potential pathogens (51). Effectively, they can modulate the adhesion of microorganisms to the oral tissue surfaces, and in consequence they contribute to the control of bacterial and fungal colonisation (51). Furthermore, mucins form complexes with other salivary proteins such as amylase, statherin, histatin and PRPs (52). These complexes may protect the proteins from enzymatic degradation or may enhance their function (27). They also facilitate daily functions such as mastication, speech and deglutition through their lubrication effect (24).

MUC5B is a high molecular weight gel forming mucin, it plays a role on the viscoelasticity of saliva (53). It has a high affinity for hydroxyapatite (54) and is a component of the acquired enamel pellicle (55). MUC7 on the other hand, is a low molecular weight monomeric mucin and has demonstrated affinity for cementum (56). It also binds to bacteria such oral Streptococci (13).

1.2.3 *Acquired Enamel Pellicle:*

1.3.3.1 *Definitions*

The acquired enamel pellicle (AEP) (10) is a thin film acquired on the surface of the teeth when exposed to the oral environment. This thin protein film can range from 0.1-1.0 µm in thickness. It is formed by a selective adsorption of many salivary proteins, but carbohydrates and lipids are also present. This protein film is involved in the demineralization-remineralization process. Because of its ideal location (between the enamel and biofilm), it will act as a natural diffusion barrier (10).

1.3.3.2 *Proteomic Analysis*

The molecular structure of the AEP has been difficult to assess, because of the very low quantity of in vivo formed pellicle that can be harvested from the tooth surface (57). It has been estimated that the amount of AEP that can be collected per tooth surface is approximately 0.5-1 µg (58). This will prevent the characterization of this protein film with classical biochemical technologies. The use of hydroxyapatite discs has been used to gain insights into the AEP (14). Therefore, in vitro and in situ studies have provided information on the affinity of salivary proteins with hydroxyapatite surfaces.

By using proteomics technologies (59), a study demonstrated that at least 200 proteins spots were detectable in AEP in a 2-D gel eletrophoretogram. But 2-D gels are limited by the dependence on protein separation, the visualization of proteins in the gel, and the labor-intensive processing of excised proteins spots. Mass spectrometric analysis (LC ESI MS/MS), in another hand, can generate a protein profile and sequence information. This allows a direct analysis of extremely

complex biological samples (14) and helps to characterize the peptides down to the femtomole level (14).

One of the persistent challenges in saliva proteomics is the collection and the storing of saliva under conditions that maintain protein structure. Because we need minimal proteolysis, deglycosylation and dephosphorylation prior to proteomic analysis (34), is important to keep the samples on ice during saliva collection and to store the samples at -80ºC (34).

Furthermore, because protein concentrations change depending on different factors (60), standardization of collection conditions is crucial for achieving reliable identification of salivary proteins (34).

1.3.3.3 *Composition and Function of AEP*

AEP has multiple functions such as neutralizing acid production by oral bacteria, acting as a lubrication film, protecting the teeth from abrasive forces (14). Because AEP can dictate the composition of initial microbial tooth colonizers, the AEP can ultimately modulate the oral biofilm and the mature plaque (61) and can have an impact on dental caries formation (14).

Previous research reported a total of 130 different proteins/peptides in the AEP (14). These proteins comprise members of the histatin, statherin, and acidic proline-rich protein (PRP) family (14). Multiple in vitro studies report that histatins, statherins, and acidic PRPs have been shown to be among the first proteins that adsorb on the hydroxyapatite surface (45,62).

Past research (14), has also identified the origin of the proteins. They noted a low value of 14.4% of all proteins derivate from exocrine salivary secretions, 85.6% originated from non-exocrine

contributors to whole saliva (comprising cells (67.8%) and serum (17.8%)) (14). They concluded that it is possible that more proteins will be identified as salivary glandular secretions with future studies (14).

Four main groups forming the AEP have been identified in past research (14), when proteins are grouped according to their chemical properties. (Figure 1).

- Protein/protein Interaction : 28.2% ■ Unknown: 38.9%
- Calcium binding : 17.5% ■ Phosphate binding : 15.4%
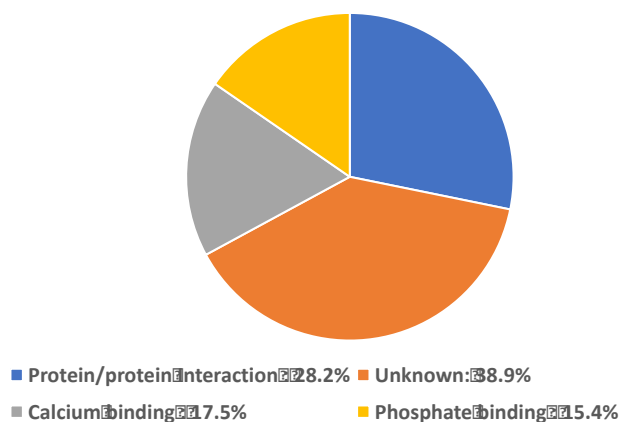
Figure 1: Classification of AEP proteins by their chemical properties. (14)

The first group is proteins that can bind calcium ions (17.5% of identified AEP proteins). They include S100 calcium binding protein family and members of the annexin family. They are considered pellicle precursor proteins due to their affinity to the calcium ions on the enamel surface. The other group (15.4%) are proteins that have a high tendency to bind to phosphate ions, such as elongation factor 2 and myosin-9, which are also in the primary protein layer because of their phosphate affinity. The third group (28.2%) identified in the literature (14) are proteins that have an interaction with other protein, such as MUC5B, which are suspected to be involved in the formation of the successive protein layers.

The other way that AEP proteins have been categorized are accoding to their biological function. Some proteins have remineralization capacities such as calgranulin and annexin families. Other proteins like cystatins (S, SA, A, B, D), lysozyme, lactotransferrin, myeloperoxidase, calgranulin A, and calgranulin B are essential for oral host defense against pathogens. These proteins are involved in the acquired immune response (11.3%) or antimicrobial activity (8.3%) (14) (Figure 2).
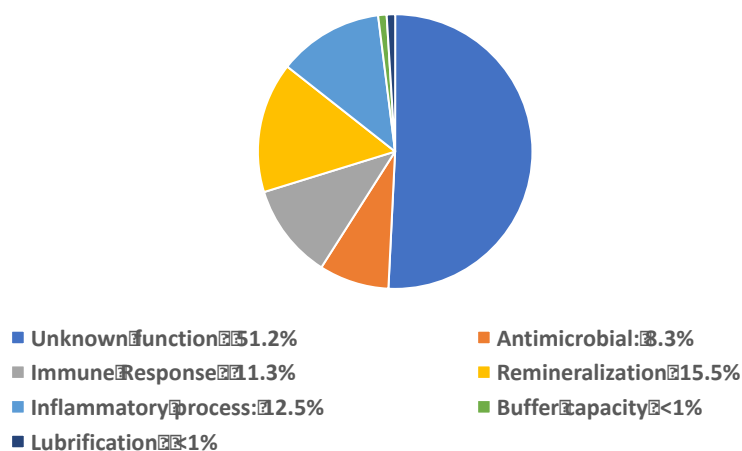
Figure 2. Classification of AEP proteins by their biological function. (14)

It has been noted that the level of gingival inflammatory disease can also have an impact on the AEP, therefore albumin, alpha-1-antitrypsin, cathepsin G, complement C3, and myeloperoxidase have been identified in the AEP components. These biomarkers for periodontal disease constitute 13% of the total number of AEP proteins (14).

1.3.3.4 *Salivary pellicles on orthodontic brackets:*

Salivary pellicles are not limited to the surface of the tooth. These are also present on the oral mucosa (12), dental appliances like orthodontic brackets (8), and even restorations and titanium implants (13).

Bacterial adhesion to the surface of orthodontic brackets involve a specific lectin-like reaction (63), electrostatic interactions and Van der Waals forces (64). Initial attachment of bacteria is an important factor that influences further colonization. The composition of the initial bacterial attachment differs depending on the surface material of the orthodontic bracket (6,21). Recent studies have found that composite brackets exhibit greater biofilm formation when compared to metallic and ceramic brackets (7). Fournier et al. (22) also found that the affinity for Streptococcus mutans was significantly lower on metallic brackets compared with the other materials.

Amylase, secretory IgA, acidic proline-rich proteins, and cystatins adhere to all kinds of brackets. However, when an electrophoresis approach was used, the differences in the gel profiles depending on the bracket material was evident, showing the selective nature of salivary protein binding (6). The largest differences observe was on the plastic brackets where acidic PRPs were more evident (6). Besides, Lee (8) reported that the pellicle components on metal brackets, were almost the same as those on the elastomeric ligature ring, with the exception that MG1 was not present on the ligature ring. Also, the degree of adhesion of cariogenic streptococci was significantly higher for bonding adhesives than for bracket materials (65).

The main factor for adhesion of Streptococci to orthodontic brackets are the bracket type, the incubation time and the saliva coating. Past studies also reported that differences can be found between the protein adsorption on the manufactured metal bracket and the raw metal material, due to surfaces properties that can change with manufacturing (8).

Besides, S. gordonii has been found to adhere to orthodontic brackets by a factor of 10 times more than S. mutans, which suggests that S. godonii can be the initial colonizer on the orthodontic brackets (6).

Higher critical surface tension, higher wettability and higher roughness of the material are variables that will have an impact on promoting biofilm adhesion (21). Surface free energy have been reported to be higher on stainless steel (SS) orthodontic brackets than ceramic brackets (21). According to that finding, bacterial adhesion should be greater on SS brackets. However, Lim et al (65) report less cariogenic streptococci adhesion on SS brackets. They concluded that a low association between surface energy and bacterial adhesion is because of others factors like surface roughness, surface charge and hydrophobicity.

Knowing that each biomaterial has unique chemical properties and surface energies, we suspect that proteins will bind differently depending on the properties of the orthodontic brackets.

1.2.4 **Composition of Orthodontic Brackets:**

1.2.4.1 *Metallic orthodontic brackets:*

There are different materials used for manufacturing orthodontic brackets including metals, plastics and ceramics. Stainless steel brackets are commonly used (66) because they have appropriate physical properties, good corrosion resistance and are affordable. Stainless steel is available as type 304, 316 and 17-4 PH SS. Most orthodontic (66) brackets are made from AISI type 304L SS, which contains 18-20% chromium and 8-10% nickel. They also have a small amount of manganese and silicon, plus a low carbon content (0.03% and less). Some manufacturers use type 316L SS, with higher nickel content, 2-3 % molybdenum, and a lower carbon content for better welding characteristics (66). Table 1 represent common elements documented by an orthodontic company for the composition of their SS orthodontic brackets.

Furthermore, the base and the wings of the brackets are mostly austenitic-type stainless steel alloys (303L, 304L, 316L, PH-14-4) and Titanium can also been found (67). The mesh is attached to the base by using brazing methods for stainless steel orthodontic brackets. Brazing fillers alloys need to be used between the bracket base and wing interface. Most SS alloys can be brazed with several different filler metal families, including: Silver, Nickel, Copper, and Gold (67).

Table 1: Composition of SS orthodontic brackets (reported by AO company)

Components	% by Weight
Silicon, Si	0 to 1.0
Manganese, Mn	0 to 2.0
Chromium, Cr	13 to 23

Nickel, Ni	3 to 14
Molybdenum, Mo	0.5 to 3
Copper, Cu	1.25 to 5
Niobium, Nb	0.15 to 0.45
Iron, Fe	50-80

Others elements may be present such as Carbon, Sulfur and Phosphorus. These are not hazardous or below 0.1% by weight.

The metallic brackets are fabricated by three main methods: casting, metal injection molding (MIM), and milling (68). The most recent technique is MIM, which is less expensive compared to the two others techniques. However, the best precision of bracket slot size is accomplished by milling the slot of a cast bracket (72).

1.2.4.2 *Ceramic Orthodontic brackets*

Aesthetics has become an important aspect when patients choose to have braces. Ceramic brackets are often used, they are made of high-purity aluminum oxide, and can be available in two forms; polycrystalline and monocrystalline. The monocrystalline brackets have the advantage of containing fewer impurities and having an excellent optical clarity.

Composition of ceramic brackets has been reported to be 100% Aluminum Oxide. A previous study (70) showed a variety of structural, compositional, and topographical characteristics when they analyzed ceramic brackets from different companies. They found the presence of single-crystal aluminum oxide (Al_2O_3), polycrystalline Al_2O_3, or Al_2O_3 and silicon oxide (SiO_2). They

also reported different brackets with rough or smooth bases. The rough areas on the bases consisted of sharp crystals or spherical glass particles.

1.2.5   <u>X-Ray Photoelectron Spectroscopy (XPS)</u>

XPS is a powerful tool for understanding the nature of many different types of surfaces, it can provide abundant information about elemental distribution, thickness, and surface functionality (15). XPS can detect all elements (except hydrogen and helium) (10) and can provide information on particle sizes on the 1-20 nm scale (15). XPS probes the surface of the sample to a depth of 5-10 nanometers (10). In other words, because the electron link to the XPS only travel a certain specific distance, it can only provide a complete information about the composition of a sample near a surface region (15).

Because electrons, can travel a short distance within a material without losing energy, we can measure the surface composition of a material, this is also possible because there is a multitude of past research about how nanostructure influences the peak intensities, signal background and the binding energies of photoelectron peaks of nanostructure materials. For example, the instrument can be calibrated to give a binding energy of 83.96 eV for the Au 4f7/2 line for metallic gold and the spectrometer dispersion can be adjusted to give a binding energy of 932.62 eV for the Cu 2p3/2 line of metallic copper (10). The other elements will be relative to this calibration.

XPS on the surface of the orthodontic bracket is very relevant, because it is providing qualitative information on the elements present at the bracket surface and it is to this surface that proteins and bacteria will adhere. This adherence will potentially cause a biofilm and can initiate caries lesions on the surround areas.

1.2.6 ElectroSpray Ionization tandem Mass Spectrometry (LC-ESI-MS/MS)

Mass spectrometric analysis (LC ESI MS/MS), can generate a protein profile and sequence information and allows characterization of peptides down to the femtomole level (14). This allows a direct analysis of extremely complex biological samples (14).

A research report (28) on phosphoproteome exploration using mass spectrometry was challenging because of the dissociation of phosphate groups during collision induced dissociation fragmentation step, which will hide the location of the phosphorylation sites. One of the solutions reported in the literature is the initiation exploration of the phosphoproteome of saliva using a chemical derivatization of the phospho-serine/ threonine-containing proteins and covalent disulfide-inter-change chromatography to capture and enrich phospho-peptides followed by intensive MS analysis, where the MS/ MS data define the location of the P-Ser and/or P-Thr residues within the amino-acid sequence. That technique allows a better comprehensive study of the phosphocreatine (28,71).

1.3 BIBLIOGRAPHY

1. Heymann GC, Grauer D. A contemporary review of white spot lesions in orthodontics. J Esthet Restor Dent 2013, Apr;25(2):85-95.

2. Enaia M, Bock N, Ruf S. White-spot lesions during multibracket appliance treatment: A challenge for clinical excellence. Am J Orthod Dentofacial Orthop 2011, Jul;140(1):e17-24.

3. Cardoso AA, Lopes LM, Rodrigues LP, Teixeira JJ, Steiner-Oliveira C, Nobre-Dos-Santos M. Influence of salivary parameters in the caries development in orthodontic patients-an observational clinical study. Int J Paediatr Dent 2017, Mar 1. DOI: 10.1111/ipd.12295

4. Ryu HS, Bae IH, Lee KG, Hwang HS, Lee KH, Koh JT, Cho JH. Antibacterial effect of silver-platinum coating for orthodontic appliances. Angle Orthod 2012, Jan;82(1):151-7.

5. van Gastel J, Quirynen M, Teughels W, Pauwels M, Coucke W, Carels C. Microbial adhesion on different bracket types in vitro. Angle Orthod 2009, Sep;79(5):915-21.

6. Ahn SJ, Kho HS, Lee SW, Nahm DS. Roles of salivary proteins in the adherence of oral streptococci to various orthodontic brackets. J Dent Res 2002, Jun;81(6):411-5.

7. Brandão GA, Pereira AC, Brandão AM, de Almeida HA, Motta RR. Does the bracket composition material influence initial biofilm formation? Indian J Dent Res 2015;26(2):148-51.

8. Lee SJ, Kho HS, Lee SW, Yang WS. Experimental salivary pellicles on the surface of orthodontic materials. Am J Orthod Dentofacial Orthop 2001, Jan;119(1):59-66.

9. do Nascimento LE, Pithon MM, dos Santos RL, Freitas AO, Alviano DS, Nojima LI, et al. Colonization of streptococcus mutans on esthetic brackets: Self-ligating vs conventional. Am J Orthod Dentofacial Orthop 2013, Apr;143(4 Suppl):S72-7.

10. Siqueira WL, Bakkal M, Xiao Y, Sutton JN, Mendes FM. Quantitative proteomic analysis of the effect of fluoride on the acquired enamel pellicle. PLoS One 2012;7(8):e42204.

11. Siqueira WL, Custodio W, McDonald EE. New insights into the composition and functions of the acquired enamel pellicle. J Dent Res 2012, Dec;91(12):1110-8.

12. Bradway SD, Bergey EJ, Jones PC, Levine MJ. Oral mucosal pellicle. Adsorption and transpeptidation of salivary components to buccal epithelial cells. Biochem J 1989, Aug 1;261(3):887-96.

13. Edgerton M, Lo SE, Scannapieco FA. Experimental salivary pellicles formed on titanium surfaces mediate adhesion of streptococci. Int J Oral Maxillofac Implants 1996;11(4):443-9.

14. Siqueira WL, Zhang W, Helmerhorst EJ, Gygi SP, Oppenheim FG. Identification of protein components in in vivo human acquired enamel pellicle using LC-ESI-MS/MS. J Proteome Res 2007, Jun;6(6):2152-60.

15. Baer DR, Engelhard MH. XPS analysis of nanostructured materials and biological surfaces. Journal of Electron Spectroscopy and Related Phenomena 2010;178:415-32.

16. Featherstone JD. The science and practice of caries prevention. J Am Dent Assoc 2000, Jul;131(7):887-99.

17. Gorelick L, Geiger AM, Gwinnett AJ. Incidence of white spot formation after bonding and banding. Am J Orthod 1982, Feb;81(2):93-8.

18. Hamdan AM, Maxfield BJ, Tüfekçi E, Shroff B, Lindauer SJ. Preventing and treating white-spot lesions associated with orthodontic treatment: A survey of general dentists and orthodontists. J Am Dent Assoc 2012, Jul;143(7):777-83.

19. Balenseifen JW, Madonia JV. Study of dental plaque in orthodontic patients. J Dent Res 1970;49(2):320-4.

20. Rosenbloom RG, Tinanoff N. Salivary streptococcus mutans levels in patients before, during, and after orthodontic treatment. Am J Orthod Dentofacial Orthop 1991, Jul;100(1):35-7.

21. Eliades T, Eliades G, Brantley WA. Microbial attachment on orthodontic appliances: I. Wettability and early pellicle formation on bracket materials. Am J Orthod Dentofacial Orthop 1995, Oct;108(4):351-60.

22. Fournier A, Payant L, Bouclin R. Adherence of streptococcus mutans to orthodontic brackets. American Journal of Orthodontics and Dentofacial Orthopedics 1998;114(4):414-7.

23. Edgar WM. Saliva: Its secretion, composition and functions. Br Dent J 1992, Apr 25;172(8):305-12.

24. Humphrey SP, Williamson RT. A review of saliva: Normal composition, flow, and function. J Prosthet Dent 2001, Feb;85(2):162-9.

25. Fejerskov O, Kidd EA. Cárie dentária: A doença e seu tratamento clínico. Santos; 2005i.

26. Figueira J, Gouveia-Figueira S, Öhman C, Holgerson PL, Nording ML, Öhman A. Metabolite quantification by NMR and LC-MS/MS reveals differences between unstimulated, stimulated, and pure parotid saliva. Journal of Pharmaceutical and Biomedical Analysis 2017;140:295-300.

27. Siqueira WL, Salih E, Wan DL, Helmerhorst EJ, Oppenheim FG. Proteome of human minor salivary gland secretion. J Dent Res 2008, May;87(5):445-50.

28. Siqueira WL, Dawes C. The salivary proteome: Challenges and perspectives. Proteomics Clin Appl 2011, Dec;5(11-12):575-9.

29. Dawes C, Wood CM. The contribution of oral minor mucous gland secretions to the volume of whole saliva in man. Arch Oral Biol 1973, Mar;18(3):337-42.

30. Edgar WM. Saliva and dental health. Clinical implications of saliva: Report of a consensus meeting. Br Dent J 1990;169(3-4):96-8.

31. Rudney JD. Does variability in salivary protein concentrations influence oral microbial ecology and oral health? Crit Rev Oral Biol Med 1995;6(4):343-67.

32. Dawes C. Circadian rhythms in the flow rate and composition of unstimulated and stimulated human submandibular saliva. J Physiol 1975, Jan;244(2):535-48.

33. Cabras T, Pisano E, Boi R, Olianas A, Manconi B, Inzitari R, et al. Age-dependent modifications of the human salivary secretory protein complex. J Proteome Res 2009, Aug;8(8):4126-34.

34. Siqueira WL, Dawes C. The salivary proteome: Challenges and perspectives. PROTEOMICS-Clinical Applications 2011;5(11-12):575-9.

35. Dawes C, Macpherson LMD. The distribution of saliva and sucrose around the mouth during the use of chewing gum and the implications for the site-specificity of caries and calculus deposition. J Dent Res 1993;72(5):852-7.

36. Turner RJ, Sugiya H. Understanding salivary fluid and protein secretion. Oral Dis 2002, Jan;8(1):3-11.

37. Veerman EC, van den Keybus PA, Vissink A, Nieuw Amerongen AV. Human glandular salivas: Their separate collection and analysis. Eur J Oral Sci 1996, Aug;104(4 (Pt 1)):346-52.

38. Moss SJ. Clinical implications of recent advances in salivary research. J Esthet Dent 1995;7(5):197-203.

39. Mandel ID. The functions of saliva. J Dent Res 1987, Feb;66 Spec No:623-7.

40. Mandel ID. The role of saliva in maintaining oral homeostasis. J Am Dent Assoc 1989, Aug;119(2):298-304.

41. Levine MJ. Development of artificial salivas. Crit Rev Oral Biol Med 1993;4(3-4):279-86.

42. Oppenheim FG, Xu T, McMillian FM, Levitz SM, Diamond RD, Offner GD, Troxler RF. Histatins, a novel family of histidine-rich proteins in human parotid secretion. Isolation,

characterization, primary structure, and fungistatic effects on candida albicans. J Biol Chem 1988, Jun 5;263(16):7472-7.

43. Siqueira WL, Margolis HC, Helmerhorst EJ, Mendes FM, Oppenheim FG. Evidence of intact histatins in the in vivo acquired enamel pellicle. J Dent Res 2010, Jun;89(6):626-30.

44. McDonald EE, Goldberg HA, Tabbara N, Mendes FM, Siqueira WL. Histatin 1 resists proteolytic degradation when adsorbed to hydroxyapatite. J Dent Res 2011, Feb;90(2):268-72.

45. Gibbons RJ, Hay DI. Adsorbed salivary acidic proline-rich proteins contribute to the adhesion of streptococcus mutans JBP to apatitic surfaces. J Dent Res 1989;68(9):1303-7.

46. Xie H, Gibbons RJ, Hay DI. Adhesive properties of strains of fusobacterium nucleatum of the subspecies nucleatum, vincentii and polymorphum. Oral Microbiol Immunol 1991, Oct;6(5):257-63.

47. Bobek LA, Aguirre A, Levine MJ. Human salivary cystatin S. Cloning, sequence analysis, hybridization in situ and immunocytochemistry. Biochemical Journal 1991;278(3):627-35.

48. Lamkin MS, Oppenheim FG. Structural features of salivary function. Crit Rev Oral Biol Med 1993;4(3-4):251-9.

49. Bennick A. Salivary proline-rich proteins. Mol Cell Biochem 1982, Jun 11;45(2):83-99.

50. Bobek LA, Tsai H, Biesbrock AR, Levine MJ. Molecular cloning, sequence, and specificity of expression of the gene encoding the low molecular weight human salivary mucin (MUC7). Journal of Biological Chemistry 1993;268(27):20563-9.

51. Tabak LA, Levine MJ, Mandel ID, Ellison SA. Role of salivary mucins in the protection of the oral cavity. J Oral Pathol 1982, Feb;11(1):1-17.

52. Bruno LS, Li X, Wang L, Soares RV, Siqueira CC, Oppenheim FG, et al. Two-hybrid analysis of human salivary mucin MUC7 interactions. Biochim Biophys Acta 2005, Oct 30;1746(1):65-72.

53. Veerman EC, Valentijn-Benz M, Nieuw AA. Viscosity of human salivary mucins: Effect of ph and ionic strength and role of sialic acid. J Biol Buccale 1989;17(4):297-306.

54. Tabak LA, Levine MJ, Jain NK, Bryan AR, Cohen RE, Monte LD, et al. Adsorption of human salivary mucins to hydroxyapatite. Arch Oral Biol 1985;30(5):423-7.

55. Al-Hashimi I, Levine MJ. Characterization of in vivo salivary-derived enamel pellicle. Arch Oral Biol 1989;34(4):289-95.

56. Fisher SJ, Prakobphol A, Kajisa L, Murray PA. External radiolabelling of components of pellicle on human enamel and cementum. Arch Oral Biol 1987;32(7):509-17.

57. Siqueira WL, Oppenheim FG. Small molecular weight proteins/peptides present in the in vivo formed human acquired enamel pellicle. Arch Oral Biol 2009;54(5):437-44.

58. Yao Y, Grogan J, Zehnder M, Lendenmann U, Nam B, Wu Z, et al. Compositional analysis of human acquired enamel pellicle by mass spectrometry. Arch Oral Biol 2001;46(4):293-303.

59. Yao Y, Berg EA, Costello CE, Troxler RF, Oppenheim FG. Identification of protein components in human acquired enamel pellicle and whole saliva using novel proteomics approaches. Journal of Biological Chemistry 2003;278(7):5300-8.

60. Dawes C. Factors influencing salivary flow rate and composition. Saliva and Oral Health 1996:27-41.

61. Li J, Helmerhorst EJ, Leone CW, Troxler RF, Yaskell T, Haffajee AD, et al. Identification of early microbial colonizers in human dental biofilm. Journal of Applied Microbiology 2004;97(6):1311-8.

62. Yao Y, Lamkin MS, Oppenheim EG. Pellicle precursor proteins: Acidic proline-rich proteins, statherin, and histatins, and their crosslinking reaction by oral transglutaminase. J Dent Res 1999;78(11):1696-703.

63. Gibbons RJ. Bacterial adhesion to oral tissues: A model for infectious diseases. J Dent Res 1989, May;68(5):750-60.

64. Mozes N, Marchal F, Hermesse MP, Van Haecht JL, Reuliaux L, Leonard AJ, Rouxhet PG. Immobilization of microorganisms by adhesion: Interplay of electrostatic and nonelectrostatic interactions. Biotechnol Bioeng 1987, Aug 20;30(3):439-50.

65. Lim BS, Lee SJ, Lee JW, Ahn SJ. Quantitative analysis of adhesion of cariogenic streptococci to orthodontic raw materials. Am J Orthod Dentofacial Orthop 2008, Jun;133(6):882-8.

66. Oh KT, Choo SU, Kim KM, Kim KN. A stainless steel bracket for orthodontic application. Eur J Orthod 2005, Jun;27(3):237-44.

67. Zinelis S, Annousaki O, Eliades T, Makou M. Elemental composition of brazing alloys in metallic orthodontic brackets. Angle Orthod 2004, Jun;74(3):394-9.

68. Alavi S, Kachuie M. Assessment of the hardness of different orthodontic wires and brackets produced by metal injection molding and conventional methods. Dent Res J (Isfahan) 2017;14(4):282-7.

69. Proffit W., Fields H., Sarver D., Ackerman J., Contemporary Orthodontics, Fifth edition, Chapter 10, p 369-370

70. Eliades T, Lekka M, Eliades G, Brantley WA. Surface characterization of ceramic brackets: A multitechnique approach. Am J Orthod Dentofacial Orthop 1994, Jan;105(1):10-8.

71. Salih E, Siqueira WL, Helmerhorst EJ, Oppenheim FG. Large-scale phosphoproteome of human whole saliva using disulfide--thiol interchange covalent chromatography and mass spectrometry. Analytical Biochemistry 2010;407(1):19-33.

CHAPTER 2

Binding of Salivary Proteins to Orthodontic Brackets

INTRODUCTION

A constant concern in the orthodontic clinic is the high prevalence of active caries lesions in patients undergoing treatment. In fact, it has been noted that 30 to 70% of patients experience active caries lesions during orthodontic treatment (1,2). Since orthodontic treatment lasts for an average of two years, the composition of the protein pellicle on the bracket surface, and the consequent biofilm formation, will have an important impact on the abundance of specific oral microorganisms.

The mechanism by which proteins adhere to surfaces is heavily determined by physico-chemical properties of the material. Therefore, analyzing the nanostructure of orthodontic brackets, for example, may provide important information regarding the reasons why specific proteins may selectively adsorb to orthodontic fixed appliances. X-ray photoelectron spectrometry (XPS) is a powerful tool that gives a multitude of information about elemental distributions and surface functionality of materials (3). XPS can detect all elements (except hydrogen and helium) (4) and can provide information on particle sizes in the 1-20 nm scale (3). XPS probes the surface of the sample to a depth of 5-10 nm (4) and provides a complete profile about the atomic structure of the surface area.

Salivary pellicles are not limited to the surface of the tooth, they are also present on the surface of the oral mucosa (5), on prosthetic restorations (6), and on dental appliances like orthodontic brackets (7). The acquired enamel pellicle (AEP) is a thin protein layer formed on the tooth surface

that plays a key role in the maintenance of oral health by regulating processes such as lubrication, demineralization, and remineralization (8). In previous investigation (9), *Liquid Chromatography – ElectroSpray Ionization tandem Mass Spectrometry* (LC-ESI-MS/MS) was used to investigate the protein composition of the *in vivo* AEP. This study disclosed that this natural film contains at least 130 different proteins. Through proteomic analysis, it is possible to discover the salivary components of the AEP and understand their functions. It will be fruitful to use this advanced technology to understand the protein pellicle specific to orthodontic brackets. This will provide an awareness and understanding of the future biofilm formation.

It is well known that the level of bacterial growth on the surface of the orthodontic brackets is variable depending on the material of the bracket (10-12). Furthermore, composite brackets have been reported to attract bacterial colonization at a rate higher than any other bracket (13). Several studies have focused on the initial bacterial binding of different orthodontic brackets (7,11,14) trying to understand which material is more prone to cariogenic bacterial adhesion. However, there is little information in the literature about the protein pellicle that initially adheres to the brackets and consequently leads to biofilm formation.

The purposes of this study were to investigate the molecular composition of two types of orthodontic brackets (metallic and ceramic) as well as to characterize the composition of the acquired protein pellicle formed on the surface of the different orthodontic brackets.

MATERIALS AND METHODS

X-ray Photoelectron Spectroscopy

X-ray Photoelectron Spectroscopy (XPS) was used to atomically analyze the composition of orthodontic metallic brackets (1.1/2.1 bracket) from American Orthodontics company, ceramic brackets (1.1/2.1 bracket) from the same company and hydroxyapatite discs (5 mm dia x 1.5-1.8 mm thick Himed inc.). Each bracket and disc were cleaned 5 minutes by sonication in 800 µL distilled water. Immediately after that, one bracket of each group and one discs were incubated for 2 hours at 37°C in 800 µL MiliQ water. Subsequently, XPS atomic analysis was performed on the incubated and not incubated samples.

XPS was calibrated with the same parameters used before (4). The instrument work function was calibrated to give a binding energy (BE) of 83.96 eV for the Au 4f7/2 line for metallic gold and the spectrometer dispersion was adjusted to give a BE of 932.62 eV for the Cu 2p3/2 line of metallic copper. The Kratos charge neutralizer system was performed on all specimens. Survey scan analysis were accomplished with an area of 300x700 µm and a pass energy of 160 eV. Spectra were analyzed using CasaXPS software (version 2.3.14). Every manipulation was repeated three times in order to have triplicates.

Whole saliva collection

Ethics approval was obtained from Research Human Ethics Board of Western University (registration number IRB 00000940) and each subjects of this study received an informed consent. Whole saliva from three healthy subjects (2 females and 1 male) aged from 30-40 years old was collected in the morning between 8h45 and 9h45 under masticatory stimulation using parafilm ($25cm^2$). Subjects were not allowed to eat or drink two hours before saliva collection. Saliva samples were kept on ice to minimize protein degradation during the collection procedure. After collection, all samples were centrifuged at 14,000xg for 20 minutes at 4°C. Following the

centrifugation, whole saliva supernatant (WSS) was separated from the pellet and pooled together for the use in this experiment. The protein concentration of this pooled sample was measured by the bicinchonic acid (BCA) assay (Pierce Chemical, Rockford, IL, USA) with bovine serum albumin used as the standard. Pooled supernatant saliva (µl) was measured and each bracket was incubated in 200 µg of total protein (Appendix 1).

Incubation of Metallic and Ceramic Brackets with Human Saliva

Brackets and HA discs (4 specimens / group) were exposed to 800 µL of distilled water for 2 h at 37˚C with gentle agitation (in 24 well culture plate). Subsequently, the pre-treated brackets and HA discs were incubated for 2 h at 37˚C with WSS containing 800 µg of total protein. Immediately after protein incubation period, the HA discs and brackets were washed using distilled water to remove any weak binding salivary protein.

Harvesting of in vitro Acquired Bracket Pellicle

*Acquired Bracket Pellicle (*ABP) and *Acquired Hydroxyapatite Pellicle (*AHP) formed on each of the brackets and disc surface (n=4/ for each group) were harvested by sonication in 300 µL of solution containing 80% acetonitrile, 19.9% water and 0.1% Trifluoroacetic acid (TFA) for 5 min. This procedure was repeated three times. Because the small amount of protein that can be harvest from one group (n=3), eluted pellicle material from the same group (from the triplicates) were pooled and concentrated by a rotary evaporator, in total we pooled 12 brackets of the same group and 12 HA discs. The total protein concentration was assessed by the micro bicinchoninic acid (Micro BCA) assay (Appendix #2).

In–solution Digestion

The equivalent of 15 µg of pellicle protein was separated from each group and placed into one polypropylene microcentrifuge tube. Dried samples were re-suspended in 50 µL of 4 M urea, 10 mM DTT and 50 mM ammonium bicarbonate at pH 7.8 and incubated for 1 hour at room temperature. Afterwards, 150 µL of 50 mM ammonium bicarbonate was added to all samples, followed by 3% (w/w) trypsin (Promega, Madison, WI, USA). Thereafter, samples were incubated for 16 h at 37 °C. Finally, the samples were dried in a rotary evaporator, de-salted by C-18 ZipTip® Pipette Tips (Millipore, Billerica, MA, USA), and subjected to mass spectrometry.

Liquid Chromatography Electrospray Ionization Tandem Mass Spectrometry (LC-ESI-MS/MS)

After trypsinization, samples were subjected to nanoscale LC-ESI-MS/MS. All samples were dried by rotary evaporator and re-suspended in 15 µL of 97.5 % H_2O/2.4% acetonitrile/0.1% formic acid and then subjected to reversed-phase LC-ESI-MS/MS. Mass spectrometric analysis was carried out with nano-HPLC Proxeon (Thermo, San Jose, CA, USA), which allows in-line liquid chromatography with the capillary column, 75 µm x 10 cm (Pico TipTM EMITTER, New Objective, Woburn, MA) packed in-house using Magic C18 resin of 5 µm diameter and 200 Å pores size (Michrom BioResources, Auburn, CA) linked to mass spectrometer (LTQVelos, Thermo Scientific, San Jose, CA, USA) using an electrospray ionization in a survey scan in the range of m/z values 390–2000 tandem MS/MS. The nano-flow reversed-phase HPLC was developed with linear 80 minutes' gradient ranging from 5% to 55% of solvent B (97.5% acetonitrile, 0.1% formic acid) in 65 minutes at a flow rate of 300 nl/min with a maximum pressure of 280 bar. Electrospray voltage and the temperature of the ion transfer capillary were 1.8 kV and 250 ºC respectively. Each survey scan (MS) was followed by automated sequential selection of

seven peptides for collision-induced dissociation (CID), with dynamic exclusion of the previously selected ions.

Data Analysis

The obtained MS/MS spectra were searched against human protein databases (Swiss Prot and TrEMBL, Swiss Institute of Bioinformatics, Geneva, Switzerland, http:// expasy.org/sprot) using SEQUEST (PROTEOMS Discover 3.0, Thermo, San Jose, CA, USA). Search results were filtered for a false discovery rate of 1% employing a decoy search strategy utilizing a reverse database. Each sample is analyzed four consecutive time by the mass spectrometry, in order to have a positive identification of proteins, the same protein passing the filter score need to be identified from at least three different MS analysis from the same group in a total of four MS analyses per group.

RESULTS

XPS analysis of metallic orthodontic brackets are shown in Table 1 and Figure 1. We noticed that there is a huge variation in the percentage of identified elements on the analysis samples. The concentration of silver, iron, niobium, palladium and chromium were variable from one metallic bracket to the other (Table 1).

Proteome identification on the different surface materials incubated with distilled water showed a total of 356 proteins in HA control group (DMQ), 298 proteins in metallic orthodontic brackets (BMQ) and 156 proteins on ceramic orthodontic brackets (CBMQ) (Table 2; Figure 3).

Only 9 proteins were common on these three groups, 36 proteins were common between metallic brackets and HA discs; and 18 proteins were common between SS brackets and ceramic brackets (Table 3). The vast majority of these proteins were identified specifically in one group indicating little overlap in the acquired pellicle proteins (Figure 3). Effectively, 84% of proteins present on the HA discs are unique to this group, 74% were unique to ceramic brackets and 79% were unique to SS brackets.

Based on MS/MS ion count from each peptide/protein, the 20 most abundant proteins present on the SS bracket pellicle, 4 had an isoelectronic point lower than 6 (pI<6), 6 had a pI between 6-8 and 10 had a pI higher than 8. For the ceramic brackets, 4 proteins had a pI less than 6, 12 had a pI between 6-8 and 4 had a pI higher than 8.

The 20 most abundant proteins on each group are presented on Table 4. These proteins are selected depending on their ion count score. The higher the ion count score the higher the probability that the protein is present in the sample.

When these proteins were categorized by biological functions (Table 5), it was observed that ceramic brackets have different proteins responsible for antibacterial and antifungal properties such as immunoglobulin, S-100 and lactotransferrin when compared with HA discs and SS brackets.

Proteins responsible for remineralization of the tooth are present such as Histatin-1 for SS bracket and HA discs and protein S-100 for ceramic bracket. Statherin was also present on SS brackets. Saliva amylase, protein responsible for early plaque formation is present on ceramic brackets and

HA discs but not found on SS bracket. Inflammatory proteins such as albumin and S-100 were only found on ceramic brackets.

DISCUSSION

In this study, we characterized the atomic composition of the surface of metallic and ceramic orthodontic brackets, and identified differences among the proteins that adhere to each of the studied surfaces.

To evaluate the relationship between the surface of the material and the adherence of the proteins, XPS analysis was performed on the surface of the orthodontic brackets. The chemical composition of this surface will regulate which functional proteins species can interact with the surface (15). Therefore, this will modulate the bacteria adhesion with the molecular structure of the adsorbed protein layer (16).

While looking at the replicate experiments to analyse the surface of SS brackets, XPS results showed a high variability. This high variability on the elements may be due to the brazing process used during the fabrication of the brackets (Appendix 3).

Knowing that proteins possess different net charges, we were not surprise to see that the bracket surfaces attract proteins with positive and negative charges without preference for one over the other. The overall net charge of orthodontic brackets material is usually neutral (17,18), but we can have areas on different material that have a positive or negative charge (15). This is also reinforced by the proteome profile of the 20 most abundant proteins identified in each group, with positive and negative proteins on the surfaces of both types of brackets. However, the charge of a

protein is not the only factor that affects its interaction with a given surface. The size, structure, stability and unfolding rate of a protein plays crucial roles in their binding capacity. Furthermore, the composition of the surfaces as well as the topography, hydrophobicity and heterogeneity of the material are also factors (15) that need to be studied in the future.

In relation to protein identification, there were significant percentages of proteins that were identified specifically to each group, suggesting specificity of the protein's adsorption in relation to the surface of the bracket. As a result, biofilm formation (4) and bacterial adhesion (15) will very likely be different among the tested brackets. Because the proteins identified on the surface of the HA discs are very different from those identified on the surface of the brackets, and knowing that HA discs mimic the surface of the tooth (4), these results suggest that SS and ceramic brackets have unique protein-adsorption properties that differ from human tooth enamel. Besides finding that most proteins are unique to each bracket material, we found that, among the 20 most abundant proteins for each group, proteins responsible for antimicrobial activity, lubrication and remineralisation function are present in both bracket materials. However, inflammatory proteins and proteins responsible of dental plaque formation were found only on ceramic brackets, when the 20 most abundant proteins for each group were considered in the two different orthodontic material.

One of the proteins that was uniquely identified in the pellicle formed on the ceramic orthodontic brackets when compared with SS brackets was amylase. A previous study suggests that salivary alpha-amylase binds very selectively and with high affinity to several streptococcal species (19). This is likely to influence commensal bacterial colonization (20) and to increase the sucrase and

transferase activities of S. mutans (21). Furthermore, starch may intensify the adhesion of amylase-binding streptococci to dental pellicles and increase the formation of dental plaque (19). Our finding is consistent with a previous study that suggests that ceramic brackets show greater affinity for Streptococcus mutans when compared to metallic brackets (22).

On the other hand, mucins were found in both bracket groups. Mucins are proteins with a high carbohydrate content. MUC5B and MUC7 are the major members of the salivary mucin family (23). MUC5B is a high molecular weight gel forming mucin, has a high affinity for hydroxyapatite (24), and is a component of the acquired enamel pellicle (25). MUC7, on the other hand, is a low molecular weight monomeric mucin and demonstrated affinity for cementum (26). It also can bind to bacteria such oral Streptococci (27). Overall, mucins play an integral role in non-immune protection (28) and they can modulate the adhesion of microorganisms to the oral tissue surfaces, and in consequence they contribute to the control of bacterial and fungal colonisation(28). Furthermore, mucins form complexes with other salivary proteins such as amylase, statherin, histatin and PRPs (29). These complexes may protect the proteins from enzymatic degradation or may enhance their function (23).

Another protein family which appears to have high affinity for ceramic surfaces are cystatins. However, no cystatins were found on SS brackets (7). Cystatins possess antimicrobial activity against oral pathogens involved in periodontal diseases such as Aggregatibacter actinomycetemcomitans (30). Their function also includes the formation of the acquired pellicle through their interaction with hydroxyapatite and they play an important role in maintaining the integrity of teeth (31).

In this study, histatin 1 was identified only on SS brackets. Histatin 1 possesses strong antifungal properties against Candida albicans (32). Furthermore, modulation of mineral formation, antibacterial activity (33,34) and protection against acid injury (35) have been reported as biological functions of histatin 1.

The initial adsorption of the proteins is an important factor for further bacteria colonization. As expected, the majority of proteins are different when the orthodontic material changes. Further investigations on bacteria adhesion depending on the bracket pellicle is needed.

CONCLUSIONS

- Our research suggests that the adsorbed protein layer, and in consequence the biofilm, will be different depending on the surface of the bracket material.
- Significant differences were noted between the different types of brackets, suggesting that there is a possibility that ceramic brackets increase the susceptibility to white spot lesions and caries.
- This study opens avenues for changes in the bracket surface as a possible way to modulate the acquired bracket pellicle to our advantage.

REFERENCES

1. Heymann GC, Grauer D. A contemporary review of white spot lesions in orthodontics. J Esthet Restor Dent 2013, Apr;25(2):85-95.

2. Enaia M, Bock N, Ruf S. White-spot lesions during multibracket appliance treatment: A challenge for clinical excellence. Am J Orthod Dentofacial Orthop 2011, Jul;140(1):e17-24.

3. Baer DR, Engelhard MH. XPS analysis of nanostructured materials and biological surfaces. Journal of Electron Spectroscopy and Related Phenomena 2010;178:415-32.

4. Siqueira WL, Bakkal M, Xiao Y, Sutton JN, Mendes FM. Quantitative proteomic analysis of the effect of fluoride on the acquired enamel pellicle. PLoS One 2012;7(8):e42204.

5. Bradway SD, Bergey EJ, Jones PC, Levine MJ. Oral mucosal pellicle. Adsorption and transpeptidation of salivary components to buccal epithelial cells. Biochem J 1989, Aug 1;261(3):887-96.

6. Lin NJ. Biofilm over teeth and restorations: What do we need to know? Dental Materials 2017.

7. Lee SJ, Kho HS, Lee SW, Yang WS. Experimental salivary pellicles on the surface of orthodontic materials. Am J Orthod Dentofacial Orthop 2001, Jan;119(1):59-66.

8. Siqueira WL, Custodio W, McDonald EE. New insights into the composition and functions of the acquired enamel pellicle. J Dent Res 2012, Dec;91(12):1110-8.

9. Siqueira WL, Zhang W, Helmerhorst EJ, Gygi SP, Oppenheim FG. Identification of protein components in in vivo human acquired enamel pellicle using LC-ESI-MS/MS. J Proteome Res 2007, Jun;6(6):2152-60.

10. Ryu HS, Bae IH, Lee KG, Hwang HS, Lee KH, Koh JT, Cho JH. Antibacterial effect of silver-platinum coating for orthodontic appliances. Angle Orthod 2012, Jan;82(1):151-7.

11. van Gastel J, Quirynen M, Teughels W, Pauwels M, Coucke W, Carels C. Microbial adhesion on different bracket types in vitro. Angle Orthod 2009, Sep;79(5):915-21.

12. Ahn SJ, Kho HS, Lee SW, Nahm DS. Roles of salivary proteins in the adherence of oral streptococci to various orthodontic brackets. J Dent Res 2002, Jun;81(6):411-5.

13. Brandão GA, Pereira AC, Brandão AM, de Almeida HA, Motta RR. Does the bracket composition material influence initial biofilm formation? Indian J Dent Res 2015;26(2):148-51.

14. do Nascimento LE, Pithon MM, dos Santos RL, Freitas AO, Alviano DS, Nojima LI, et al. Colonization of streptococcus mutans on esthetic brackets: Self-ligating vs conventional. Am J Orthod Dentofacial Orthop 2013, Apr;143(4 Suppl):S72-7.

15. Dee KC, Puleo DA, Bizios R. An introduction to tissue-biomaterial interactions. Cell Mol. Biol 2004;8:419-25.

16. Latour RA. Biomaterials: Protein-surface interactions. Encyclopedia of Biomaterials and Biomedical Engineering 2005;1:270-8.

17. Balzarotti A, Bianconi A. Electronic structure of aluminium oxide as determined by x-ray photoemission. Physica Status Solidi (b) 1976;76(2):689-94.

18. Hermas AA, Nakayama M, Ogura K. Enrichment of chromium-content in passive layers on stainless steel coated with polyaniline. Electrochimica Acta 2005;50(10):2001-7.

19. Scannapieco FA, Torres GI, Levine MJ. Salivary amylase promotes adhesion of oral streptococci to hydroxyapatite. J Dent Res 1995, Jul;74(7):1360-6.

20. Nikitkova AE, Haase EM, Scannapieco FA. Taking the starch out of oral biofilm formation: Molecular basis and functional significance of salivary α-amylase binding to oral streptococci. Appl Environ Microbiol 2013, Jan;79(2):416-23.

21. Chaudhuri B, Rojek J, Vickerman MM, Tanzer JM, Scannapieco FA. Interaction of salivary alpha-amylase and amylase-binding-protein A (abpa) of streptococcus gordonii with glucosyltransferase of S. Gordonii and streptococcus mutans. BMC Microbiol 2007, Jun 25;7:60.

22. Fournier A, Payant L, Bouclin R. Adherence of streptococcus mutans to orthodontic brackets. American Journal of Orthodontics and Dentofacial Orthopedics 1998;114(4):414-7.

23. Siqueira WL, Salih E, Wan DL, Helmerhorst EJ, Oppenheim FG. Proteome of human minor salivary gland secretion. J Dent Res 2008, May;87(5):445-50.

24. Tabak LA, Levine MJ, Jain NK, Bryan AR, Cohen RE, Monte LD, et al. Adsorption of human salivary mucins to hydroxyapatite. Arch Oral Biol 1985;30(5):423-7.

25. Al-Hashimi I, Levine MJ. Characterization of in vivo salivary-derived enamel pellicle. Arch Oral Biol 1989;34(4):289-95.

26. Fisher SJ, Prakobphol A, Kajisa L, Murray PA. External radiolabelling of components of pellicle on human enamel and cementum. Arch Oral Biol 1987;32(7):509-17.

27. Edgerton M, Lo SE, Scannapieco FA. Experimental salivary pellicles formed on titanium surfaces mediate adhesion of streptococci. Int J Oral Maxillofac Implants 1996;11(4):443-9.

28. Tabak LA, Levine MJ, Mandel ID, Ellison SA. Role of salivary mucins in the protection of the oral cavity. J Oral Pathol 1982, Feb;11(1):1-17.

29. Bruno LS, Li X, Wang L, Soares RV, Siqueira CC, Oppenheim FG, et al. Two-hybrid analysis of human salivary mucin MUC7 interactions. Biochim Biophys Acta 2005, Oct 30;1746(1):65-72.

30. Ganeshnarayan K, Velliyagounder K, Furgang D, Fine DH. Human salivary cystatin SA exhibits antimicrobial effect against aggregatibacter actinomycetemcomitans. J Periodontal Res 2012, Oct;47(5):661-73.

31. Lamkin MS, Oppenheim FG. Structural features of salivary function. Crit Rev Oral Biol Med 1993;4(3-4):251-9.

32. Oppenheim FG, Xu T, McMillian FM, Levitz SM, Diamond RD, Offner GD, Troxler RF. Histatins, a novel family of histidine-rich proteins in human parotid secretion. Isolation, characterization, primary structure, and fungistatic effects on candida albicans. J Biol Chem 1988, Jun 5;263(16):7472-7.

33. Raj PA, Edgerton M, Levine MJ. Salivary histatin 5: Dependence of sequence, chain length, and helical conformation for candidacidal activity. J Biol Chem 1990, Mar 5;265(7):3898-905.

34. Edgerton M, Koshlukova SE. Salivary histatin 5 and its similarities to the other antimicrobial proteins in human saliva. Adv Dent Res 2000, Dec;14:16-21.

35. Siqueira WL, Margolis HC, Helmerhorst EJ, Mendes FM, Oppenheim FG. Evidence of intact histatins in the in vivo acquired enamel pellicle. J Dent Res 2010, Jun;89(6):626-30.

Chapter 3

"Key aspects for the future work"

Orthodontic brackets serve as loci for biofilm formation and create new locations for plaque retention, which increase dangerously the chances of tooth demineralization (1). In consequence, the incidence of white spot lesions was reported to be 60% in orthodontic patients (2). In some cases, orthodontic treatment must be interrupted, because of lack of oral hygiene and high prevalence of decay in the mouth, causing perfectly straight teeth with compromised oral health. If clinicians want to minimize the risk of caries and white spot lesions, it is important to emphasize on investigating protein adherence on different orthodontic materials, since proteins are the first to adsorb onto the surface of the bracket, saturating completely the surface within seconds to minutes. Later, living cells, including bacteria, will contact and interact with the molecular structure of the adsorbed protein layer forming the biofilm (3). Effectively, initial bacterial attachment is mediated by the protein pellicle composition, which can modify the surface chemistry and have an impact on bacterial adhesion (4). Therefore, understanding the modulation of the acquired pellicle when the surface of the orthodontic brackets change allows us to have a better knowledge on the future biofilm formation.

Our research suggests that the adsorbed protein layer and in consequence the biofilm will be different depending on the surface of the material because most of the proteins present on the acquired pellicle were identified specifically to each group, indicating little overlap in the acquired pellicle proteins. Furthermore, significant differences on the type of proteins responsible of dental plaque formation and maturation like amylase (5) were noted between the different types of brackets. When the 20 most abundant proteins from each group were analyzed, our results showed

that Alpha-amylase was present only on ceramic brackets. Prior studies demonstrated that salivary alpha-amylase binds very selectively and with high affinity to several streptococcal species (5). This is likely to influences commensal bacterial colonization (6) and to increase the sucrase and transferase component activities of S. mutans (7). Furthermore, starch may intensify the adhesion of amylase-binding streptococci to amylase in dental pellicles and increase the formation of dental plaque (5). This can be related to past literature that suggests that ceramic brackets have more affinity for Streptococcus mutants then metallic brackets (8).

Because of the high demand of esthetic brackets, orthodontic materials have improved drastically on that area. However, few literature is concentrated on new ceramic and metallic brackets treated or coated with material that will decreased white spot lesions and caries. On the other hand, in the implantology field we found an evolution on multiple treated surfaces in the past 25 years (9). Surface energy, charge, composition and morphology is amongst the physicochemical characteristic which were modified during the years for a better stability and biocompatibility of the implants (9). It will be interesting in the future to have orthodontic brackets (SS and ceramic) coated with materials that absorb proteins able to repulse bacteria responsible for tooth demineralization.

For further control of cariogenic plaque, it will also be interesting to have orthodontic accessories, such as powerchains and elastics, with same physical properties but with chemical components that help decrease cariogenic biofilm accumulation and maturation. For the moment, research has reported a possible coating on the surface of SS orthodontic brackets that released sufficient Silver (Ag) ions when immersed in phosphate-buffered saline which shows significant antimicrobial potency against Streptococcus mutans and Aggregatibacter actinomycetemcomitans strains (10).

Some authors also report fluoride-releasing materials (11,12) to reduce the risk of developing a white spot lesions around the orthodontic bracket. However, Nascimento concluded by warning orthodontists that there is limited evidence to support the use of fluoride-releasing materials in order to prevent white spot lesions development (11). Furthermore, a review on prevention and treatment of white spot lesions mentions that multiple recent narrative and systematic reviews have failed to present sufficient evidence for most preventive measures against white spot lesions, except for the topical application of fluoride-containing products (13). However, fluoride mouthwash and fluoride toothpaste have the disadvantage to be patient-dependant. It has been shown that only 13% of the patients comply fully with the fluoride recommendations (14). These data highlight the importance of developing modified fluoride-releasing materials instead of depending on the "good hygiene" of our patients.

New area of research, including proteomics allows us to study the protein pellicle with precision. This new science is very promising to help us understand better the relationship between oral biofilm and oral disease with the objective of providing information on potential targets for biofilm interruption and advance with new antimicrobial materials.

This study, is very relevant because it opens avenues on the not yet characterized changes on the bracket surface and the possible ways to modulate the acquired bracket pellicle in our advantage. In a near future, we hope to see new materials able to prevent cariogenic biofilm adhesion, and to attract proteins that can promote tooth remineralization to the bracket surface. This will have a big impact on the oral health of orthodontic patients.

REFERENCES

1. van Gastel J, Quirynen M, Teughels W, Pauwels M, Coucke W, Carels C. Microbial adhesion on different bracket types in vitro. Angle Orthod 2009, Sep;79(5):915-21.

2. Enaia M, Bock N, Ruf S. White-spot lesions during multibracket appliance treatment: A challenge for clinical excellence. Am J Orthod Dentofacial Orthop 2011, Jul;140(1):e17-24.

3. Latour RA. Biomaterials: Protein-surface interactions. Encyclopedia of Biomaterials and Biomedical Engineering 2005;1:270-8.

4. Lin NJ. Biofilm over teeth and restorations: What do we need to know? Dental Materials 2017.

5. Scannapieco FA, Torres GI, Levine MJ. Salivary amylase promotes adhesion of oral streptococci to hydroxyapatite. J Dent Res 1995, Jul;74(7):1360-6.

6. Nikitkova AE, Haase EM, Scannapieco FA. Taking the starch out of oral biofilm formation: Molecular basis and functional significance of salivary α-amylase binding to oral streptococci. Appl Environ Microbiol 2013, Jan;79(2):416-23.

7. Chaudhuri B, Rojek J, Vickerman MM, Tanzer JM, Scannapieco FA. Interaction of salivary alpha-amylase and amylase-binding-protein A (abpa) of streptococcus gordonii with glucosyltransferase of S. Gordonii and streptococcus mutans. BMC Microbiol 2007, Jun 25;7:60.

8. Fournier A, Payant L, Bouclin R. Adherence of streptococcus mutans to orthodontic brackets. American Journal of Orthodontics and Dentofacial Orthopedics 1998;114(4):414-7.

9. Biotechnology-Molecular Studies and Novel Applications for Improved Quality of Human Life. InTech; 2012.

10. Ryu HS, Bae IH, Lee KG, Hwang HS, Lee KH, Koh JT, Cho JH. Antibacterial effect of silver-platinum coating for orthodontic appliances. Angle Orthod 2012, Jan;82(1):151-7.

11. Nascimento PL, Fernandes MT, Figueiredo FE, Faria-E-Silva AL. Fluoride-Releasing materials to prevent white spot lesions around orthodontic brackets: A systematic review. Braz Dent J 2016;27(1):101-7.

12. Srivastava K, Tikku T, Khanna R, Sachan K. Risk factors and management of white spot lesions in orthodontics. J Orthod Sci 2013, Apr;2(2):43-9.

13. Bergstrand F, Twetman S. A review on prevention and treatment of post-orthodontic white spot lesions - evidence-based methods and emerging technologies. Open Dent J 2011;5:158-62.

14. Geiger AM, Gorelick L, Gwinnett AJ, Benson BJ. Reducing white spot lesions in orthodontic populations with fluoride rinsing. Am J Orthod Dentofacial Orthop 1992, May;101(5):403-7.

Table 1. Atoms % of molecules on the surface of A) HA Discs; (ND) HA discs without incubation, (DW) HA discs incubated in distilled water, B) SS orthodontic brackets; (NB) SS brackets without incubation, (BW) SS bracket incubated in distilled water, C) ceramic brackets; (NCB) C brackets without incubation, (CBW) C brackets incubated in distilled water. Means ±SD

A)

	DW
I	0.1 ±0.0
Ca	21.4±0.2
Cu	0.8 ±0.1
F	0.2 ±0.3
Na	0.5±0.4
O	62.4 ±0.5
P	14.7±0.8
Ratio Ca/P	1.5±0.1

B)

	BW
Ag	10.6 ±0.8
B	5.3±0.4
Cr	12.8±1.3
Cu	1.6±0.2
Fe	3.4±0.7
N	5.9±1.1
Na	0.7±0.5
Nb	1.5±0.2
O	55.0±0.4
Pd	0.9±0.0
S	1.1±0.3
Si	1.2±0.4

C)

	CBW
Al	28.3±1.22
Ca	0.1±0.04
Cl	0.1±0.14
F	0.1±0.10
K	0.7±0.6
N	0.8±0.22
Na	0.4±0.18
O	67.2±1.61
S	–
Si	2.3±0.32

Table 2. Total pellicle proteins present on metallic brackets surface (BMQ), ceramic brackets (CBMQ) and HA discs (DMQ)			
BMQ			
Accession Number	Description (protein name)	Ion count score	MW [kDa]
P13645	Keratin, type I cytoskeletal 10	263.77	58.79
A0A0A0MTS7	Titin	175.26	3992.17
H6VRF8	Keratin 1	175.13	66.01
P02814	Submaxillary gland androgen-regulated protein 3B	105.99	8.18
P35527	Keratin, type I cytoskeletal 9	96.87	62.03
P35908	Keratin, type II cytoskeletal 2 epidermal	96.10	65.39
M0R088	Serine/arginine repetitive matrix protein 1	59.52	78.09
Q6ZRI6	Uncharacterized protein C15orf39	56.38	110.60
P15515	Histatin-1	54.31	6.96
B3KXW2	cDNA FLJ46178 fis, clone TESTI4003944	50.78	141.62
F5GZK2	Collagen alpha-1(XXI)	49.95	99.23
Q8WXI7	Mucin-16	47.89	1518.24
Q96RT6	cTAGE family member 2	41.43	85.23
B4DRU6	cDNA FLJ54657, highly similar to Keratin, type II cytoskeletal 6A	39.88	58.50
Q92954	Proteoglycan 4	39.63	150.98
Q5CZC0	Fibrous sheath-interacting protein 2	34.44	780.12
B4DVQ0	cDNA FLJ58286, highly similar to Actin, cytoplasmic 2	33.09	37.32
A0A0J9YYJ7	Unconventional myosin-XVB	32.86	79.47
A2A2V2	RNA-binding protein 34	32.18	45.89
B3KNX8	cDNA FLJ30689 fis, clone FCBBF2000566	30.34	84.45
E9PAV3	Nascent polypeptide-associated complex subunit alpha, muscle-specific form	30.12	205.29
Q7Z5P9	Mucin-19	30.11	804.77
Q6P4R9	SASH1 protein	25.96	134.74
Q01546	Keratin, type II cytoskeletal 2 oral	25.07	65.80
Q9C0F0	Putative Polycomb group protein ASXL3	22.60	241.77
P02808	Statherin	22.41	7.30
O60382	KIAA0324	22.20	191.19
A0A0U1RRH1	Ryanodine receptor 3	20.06	550.47
Q3SY84	Keratin, type II cytoskeletal 71	19.15	57.26
Q5T3J3	Ligand-dependent nuclear receptor-interacting factor 1	17.82	84.52

A8K781	cDNA FLJ75299	17.80	47.29
T1R7N3	MUC5AC	16.90	413.62
Q5VST9	Obscurin	16.86	867.94
Q5SYE7	NHS-like protein 1	16.58	170.56
A0A024RBF1	Protein phosphatase 1, regulatory (Inhibitor) subunit 12A, isoform CRA_a	16.55	101.54
A4UGR9	Xin actin-binding repeat-containing protein 2	16.29	382.06
Q86UP3	Zinc finger homeobox protein 4	16.13	393.48
H7BY37	Histone-lysine N-methyltransferase 2C	16.09	269.44
Q2KHM5	CENPJ protein	16.02	129.87
G8GEI5	Coagulation factor VIII	15.77	8.36
B7ZA42	cDNA, FLJ79056	15.51	77.19
Q9NSI6	Bromodomain and WD repeat-containing protein 1	15.39	262.77
Q9ULU4	Protein kinase C-binding protein 1	15.27	131.61
K7ERE3	Keratin, type I cytoskeletal 13	15.18	45.23
C9JE98	Nuclear receptor corepressor 2	15.05	267.88
Q86YZ3	Hornerin	14.75	282.23
A0A0B4J1Z0	COBL-like 1, isoform CRA_a	14.40	46.75
A0A087WZ32	Pleckstrin homology domain-containing family A member 2	14.39	41.18
B8XCX8	EPC1/ASXL2b fusion protein	13.90	201.73
B4DDN6	cDNA FLJ54422	13.75	71.96
E9PPJ1	Kinetochore scaffold 1	13.69	195.52
Q9UJT9	F-box/LRR-repeat protein 7	13.55	54.54
A0A1U9XBF2	MDC1	13.35	226.47
B4E1A2	Gamma-aminobutyric acid (GABA) A receptor, alpha 5, isoform CRA_a	13.31	38.99
P54259	Atrophin-1	13.22	125.34
Q8WXG9	G-protein coupled receptor 98	13.19	692.64
B4DH81	cDNA FLJ61250	13.18	93.45
Q96HA1	Nuclear envelope pore membrane protein POM 121	13.17	127.64
P51826	AF4/FMR2 family member 3	13.15	133.39
A0A1U9XBE1	MDC1	13.06	226.46
A0A1B0GWE0	Dedicator of cytokinesis protein 7 (Fragment)	13.05	139.52
Q66PJ3	ADP-ribosylation factor-like protein 6-interacting protein 4	12.93	44.89
Q15751	Probable E3 ubiquitin-protein ligase HERC1	12.90	531.89
Q9NXV6	CDKN2A-interacting protein	12.83	61.09
Q8N7X4	Melanoma-associated antigen B6	12.62	43.96
A0A087WW76	Rho GTPase-activating protein 21	12.42	155.89
B5M450	Anion exchange protein	12.40	135.22

Q8IVL0	Neuron navigator 3	12.32	255.49
Q6LEQ8	LTG9/MLLT3 protein	11.59	38.09
Q96T58	Msx2-interacting protein	11.45	402.00
Q6ZU65	Ubinuclein-2	11.33	146.00
J3KQ96	Treacle protein	11.25	144.04
Q6PII6	TMF1 protein	11.25	58.35
A0A1U9X7B3	BRD2	11.21	74.71
Q7Z7G8	Vacuolar protein sorting-associated protein 13B	11.11	448.38
O75592	E3 ubiquitin-protein ligase MYCBP2	11.08	509.76
B2RAG9	Mediator of RNA polymerase II transcription subunit 1	11.08	166.54
Q9UPN3	Microtubule-actin cross-linking factor 1, isoforms 1/2/3/5	11.06	837.79
Q5KU20	G-protein coupled receptor	11.05	102.05
Q6N055	Putative uncharacterized protein DKFZp686O11112	11.03	35.54
H3BM45	Ankyrin repeat and fibronectin type-III domain-containing protein 1	10.87	129.87
Q59H94	Gamma filamin variant	10.69	142.73
F4MH51	Ubiquitously transcribed tetratricopeptide repeat protein Y-linked transcript variant 60	10.41	147.07
D6RD46	LIM and calponin homology domains-containing protein 1	10.35	109.87
B7Z2P9	E3 ubiquitin-protein ligase	10.34	96.34
A0A1W2PR28	IQ motif and SEC7 domain-containing protein 2	10.31	127.90
Q96JG9	Zinc finger protein 469	10.29	409.95
Q9BTM2	C2CD2L protein	10.17	28.22
Q9NZR2	Low-density lipoprotein receptor-related protein 1B	10.17	515.16
O95996	Adenomatous polyposis coli protein 2	10.09	243.80
B4DJT3	cDNA FLJ54498, weakly similar to Mucin-like protein 1	10.04	67.74
A0A024RAN2	Calpastatin, isoform CRA_a	10.03	86.56
B7ZLW1	CAMSAP1 protein	10.01	163.16
Q5T4S7	E3 ubiquitin-protein ligase UBR4	9.99	573.48
F8VZ81	TBC1 domain family member 30	9.99	71.78
X6R7H2	Peroxisome proliferator-activated receptor gamma coactivator-related protein 1	9.98	69.06
Q53F67	Kringle-containing transmembrane protein 2 isoform b variant	9.96	44.42
Q6ZS56	cDNA FLJ45819 fis, clone NT2RP8001363	9.96	66.96
Q96F05	Uncharacterized protein C11orf24	9.93	46.07
Q8IVF2	Protein AHNAK2	9.91	616.24
A0A087WXN9	MTSS1-like protein	9.90	79.75
Q9UL49	Transcription factor-like 5 protein	9.89	52.66

H0YLN8	Transient receptor potential cation channel subfamily M member 7	9.87	212.49
B3KPL9	cDNA FLJ31930 fis, clone NT2RP7006162	9.85	47.82
A0A0G2JN73	Diffuse panbronchiolitis critical region protein 1	9.84	56.31
Q05CT8	NEDD1 protein	9.83	57.47
A0A1B0GUS7	Protein unc-13 homolog B	9.79	483.83
Q9NR48	Histone-lysine N-methyltransferase ASH1L	9.76	332.58
Q53QN9	Putative uncharacterized protein ABCG5	9.76	60.84
A0A1B0GV45	Unconventional myosin-XVIIIa	9.74	49.69
I0B0K8	Truncated profilaggrin	9.72	430.16
B7Z526	cDNA FLJ59292	9.71	85.62
H7C1L9	E3 ubiquitin-protein ligase TRIP12	9.69	22.41
Q59G99	Dishevelled 1 isoform a variant	9.69	40.28
E7EPM4	Mucin-17	9.64	425.29
H3BR17	E3 ubiquitin-protein ligase TRAF7	9.63	15.86
B4E392	cDNA FLJ52602, highly similar to Pinin	9.63	49.11
Q9UHR4	Brain-specific angiogenesis inhibitor 1-associated protein 2-like protein 1	9.63	56.85
Q92610	Zinc finger protein 592	9.62	137.44
A0A1W2PQJ7	Retinoic acid-induced protein 1	9.54	183.82
P46013	Proliferation marker protein Ki-67	9.54	358.47
K7EMR9	Dynamin-2	9.53	18.20
Q9HCK8	Chromodomain-helicase-DNA-binding protein 8	9.52	290.34
F5H101	Nucleolar protein 8	9.48	121.52
P56555	Down syndrome critical region protein 4	9.37	12.95
Q8NA90	cDNA FLJ35733 fis, clone TESTI2003277	9.36	29.45
A8KAI3	cDNA FLJ77394	9.09	57.44
H3BLS7	Vacuolar protein sorting-associated protein 13D	8.99	356.81
A0A024QZW7	Nucleoporin 153kDa, isoform CRA_a	8.92	153.87
B3KR92	cDNA FLJ33882 fis, clone CTONG2007175	8.84	61.73
A8K8M7	cDNA FLJ76439	8.82	53.73
Q5VWG9	Transcription initiation factor TFIID subunit 3	8.76	103.52
Q14686	Nuclear receptor coactivator 6	8.73	219.01
A0A1W2PQW2	Voltage-dependent T-type calcium channel subunit alpha-1H	8.59	178.43
Q9UPU5	Ubiquitin carboxyl-terminal hydrolase 24	8.53	294.18
P13611	Versican core protein	8.46	372.59
P25054	Adenomatous polyposis coli protein	8.36	311.45
Q02388	Collagen alpha-1(VII)	8.32	295.04
A0A0A0MS79	Nck-associated protein 5	8.26	208.35

Q9UIF8	Bromodomain adjacent to zinc finger domain protein 2B	8.26	240.31
A0A140VJJ5	Testicular tissue protein Li 69	8.13	119.70
Q8WVS4	WD repeat-containing protein 60	8.07	122.50
A0A0U1RQK4	[Protein ADP-ribosylarginine] hydrolase-like protein 1	7.97	211.69
Q8NB66	Protein unc-13 homolog C	7.86	250.75
Q7Z2Y8	Interferon-induced very large GTPase 1	7.83	278.87
F8WDA1	5'-AMP-activated protein kinase subunit gamma-2	7.80	24.62
B5A965	Soluble FGFR4 variant 2	7.48	48.62
H7BY35	Ryanodine receptor 2	7.37	562.25
Q9UKN1	Mucin-12	7.25	557.83
A0A1S5UZ29	Kalirin	7.24	269.17
H0YL16	Serine/threonine-protein kinase PAK 6	7.21	30.72
Q86XZ4	Spermatogenesis-associated serine-rich protein 2	7.20	59.51
Q5T0Z8	Uncharacterized protein C6orf132	7.18	123.96
A8K8U1	cDNA FLJ77762	7.17	136.23
Q9NYB5	Solute carrier organic anion transporter family member 1C1	7.15	78.65
D3DWL9	Cleavage and polyadenylation specific factor 1, 160kDa, isoform CRA_a	7.11	151.89
Q9NT22	EMILIN-3	7.08	82.60
B1WB49	BDP1 protein	7.04	293.25
Q6WKZ4	Rab11 family-interacting protein 1	6.96	137.08
Q8WYX4	Putative uncharacterized protein pp11662	6.94	21.03
P49916	DNA ligase 3	6.94	112.83
O60307	Microtubule-associated serine/threonine-protein kinase 3	6.93	143.05
E9PL24	Myomegalin	6.88	126.87
H7BZB4	C2 domain-containing protein 3	6.88	86.23
B4E345	cDNA FLJ50374, weakly similar to Protein groucho	6.86	61.71
Q9UF83	Uncharacterized protein DKFZp434B061	6.86	59.38
D3DR86	Nuclear factor of kappa light polypeptide gene enhancer in B-cells 2 (P49/p100)	6.84	44.23
Q5M9Q1	NKAP-like protein	6.83	46.28
Q9Y5S2	Serine/threonine-protein kinase MRCK beta	6.83	194.19
A2SY06	MAP/microtubule affinity-regulating kinase 3	6.81	36.68
Q9NRK6	ATP-binding cassette sub-family B member 10, mitochondrial	6.80	79.10
P98169	Zinc finger X-linked protein ZXDB	6.80	84.74
A0A075B6G6	Filamin A interacting protein 1, isoform CRA_c	6.80	127.13
Q9HCM3	UPF0606 protein KIAA1549	6.80	210.63
Q969K3	E3 ubiquitin-protein ligase RNF34	6.80	41.61
H0YC33	La-related protein 1	6.79	20.88

B9ZVN9	DNA-directed RNA polymerase subunit	6.78	187.69
A8KAY2	Fibrillin 3	6.76	300.12
B4E223	cDNA FLJ52075	6.76	68.46
Q6ZMZ1	cDNA FLJ16568 fis, clone TESOP2000390	6.74	52.00
C9J164	Ras-associated and pleckstrin homology domains-containing protein 1	6.72	67.14
A0A024R7D8	Ral guanine nucleotide dissociation stimulator-like 3, isoform CRA_a	6.72	51.08
Q8NAV8	cDNA FLJ34691 fis, clone MESAN2000909	6.72	64.30
B4DGV8	cDNA FLJ54286	6.71	19.45
H7C189	Ubiquitin carboxyl-terminal hydrolase 4	6.70	69.51
Q8N0Z3	Spindle and centriole-associated protein 1	6.69	96.21
Q9UJ55	MAGE-like protein 2	6.69	132.74
Q96KW2	POM121-like protein 2	6.69	109.84
Q5T1H1	Protein eyes shut homolog	6.68	350.57
A8MXZ3	Keratin-associated protein 9-1	6.68	26.31
Q6DKI7	Transmembrane protein PVRIG	6.68	34.32
P47989	Xanthine dehydrogenase/oxidase	6.67	146.33
B2RTX2	Palladin, cytoskeletal associated protein	6.67	121.97
A0A0A0MS59	Helicase SRCAP	6.66	315.42
A0A090N8E5	Similar to OG-2 homeodomain protein-like similar to U65067 (PID:g1575526)	6.65	52.71
Q0IIP3	C20orf194 protein	6.65	102.18
A0A024RAL3	Zinc finger, FYVE domain containing 16, isoform CRA_a	6.65	168.74
M0R219	Liprin-alpha-4	6.64	20.44
Q53TT7	Putative uncharacterized protein ALS2CR3	6.63	97.93
L8E9Z3	Alternative protein HRC	6.62	34.32
O43149	Zinc finger ZZ-type and EF-hand domain-containing protein 1	6.62	330.86
Q6ZWP8	Inactive rhomboid protein	6.62	80.36
M0R0C4	Dystrobrevin alpha	6.60	18.64
A0A5B4	T-cell receptor beta variable 20-1	6.60	12.20
V9GZ26	Protein FAM110A	6.60	19.68
M0R0F4	Atypical kinase COQ8B, mitochondrial	6.60	12.11
J3QKX6	SWI/SNF-related matrix-associated actin-dependent regulator of chromatin subfamily E member 1	6.60	14.60
P35900	Keratin, type I cytoskeletal 20	6.59	48.46
A0A1S5UYZ7	Rap guanine nucleotide exchange factor 1	6.56	120.16
Q13233	Mitogen-activated protein kinase kinase kinase 1	6.56	164.37
Q8IYJ2	Uncharacterized protein C10orf67, mitochondrial	6.55	63.62

B2RB68	cDNA, FLJ95336	6.55	67.80
B4DQR1	cDNA FLJ55241	6.55	22.93
Q4EW05	Rhesus blood group D antigen	6.55	6.03
B4DLJ7	cDNA FLJ59334	6.54	57.18
A0A087WUH9	Serine/threonine-protein kinase PLK	6.53	76.60
Q9ULL0	Acrosomal protein KIAA1210	6.52	186.90
B3KVV3	cDNA FLJ41584 fis, clone CTONG2020445	6.52	72.29
E9PCY0	Dynactin subunit 1	6.52	19.44
Q9Y4F1	FERM, RhoGEF and pleckstrin domain-containing protein 1	6.52	118.56
A0A024R2Y4	Bassoon (Presynaptic cytomatrix protein), isoform CRA_a	6.52	416.24
Q86YS7	C2 domain-containing protein 5	6.50	110.38
D3DPE6	Wiskott-Aldrich syndrome protein interacting protein, isoform CRA_a	6.49	50.27
O60293	Zinc finger C3H1 domain-containing protein	6.48	226.21
H3BN61	Doublesex- and mab-3-related transcription factor 1	6.48	23.16
P39880	Homeobox protein cut-like 1	6.47	164.09
J3KSW8	Myosin phosphatase Rho-interacting protein	6.45	95.87
H0Y797	Thyrotroph embryonic factor	6.45	20.00
A5XEH6	WNK lysine deficient protein kinase 1	6.44	7.71
E9PM59	TATA box-binding protein-associated factor RNA polymerase I subunit D	6.44	25.03
H0YEU1	CD44 antigen	6.43	27.26
C9JR56	DNA-binding protein SATB	6.43	75.99
H0YGW3	Protein FAM13C	6.43	15.38
Q96RV3	Pecanex-like protein 1	6.43	258.51
Q4KWH8	1-phosphatidylinositol 4,5-bisphosphate phosphodiesterase eta-1	6.43	189.10
J3KNV1	Zinc finger protein 292	6.43	304.02
L8E767	Alternative protein RNF222	6.42	19.45
F5GX59	Zonadhesin	6.41	282.23
F5H514	RAS guanyl-releasing protein 1	6.41	90.31
O75113	NEDD4-binding protein 1	6.40	100.32
C9JFF0	Kinesin-like protein KIF26A	6.40	180.04
Q59FH1	Transformation/transcription domain-associated protein variant	6.39	405.56
H0Y8C9	ATP-binding cassette sub-family A member 2	6.38	118.05
A0A087WYF1	Laminin subunit alpha-2	6.38	343.20
A9UF07	BCR/ABL fusion protein isoform Y5	6.37	196.45

B4DHI4	cDNA FLJ60536, highly similar to Death-associated protein kinase 1 (EC 2.7.11.1) OS=Homo sapiens PE=2 SV=1 - [B4DHI4_HUMAN]	6.36	159.96
D3DSU3	Kinesin family member 13B, isoform CRA_a	6.36	174.69
F5H3X8	Poly [ADP-ribose] polymerase	6.36	55.11
Q53F19	Nuclear cap-binding protein subunit 3	6.35	70.55
Q6R743	MHC class I antigen	6.34	41.60
P98088	Mucin-5AC	6.34	585.20
Q7LGH1	KIAA0480 protein	6.32	146.90
B5BUB1	RuvB-like helicase	6.31	50.18
Q9NX53	Exonuclease mut-7 homolog, isoform 5	6.29	26.34
Q59F85	Glucose phosphate isomerase variant	6.28	55.65
Q53GZ4	Leucine rich repeat containing 5 variant	6.26	76.80
P61129	Zinc finger CCCH domain-containing protein 6	6.26	131.59
B4E1I2	cDNA FLJ61037, highly similar to Intraflagellar transport 88 homolog	6.26	12.38
Q8N3N3	Putative uncharacterized protein DKFZp762L056	6.26	89.64
Q59EC9	Glyceronephosphate O-acyltransferase variant	6.25	78.54
L8ECB8	Alternative protein NR5A1	6.25	19.48
Q9C0D2	Centrosomal protein of 295 kDa	6.22	295.00
Q0PNF2	FEX1	6.14	275.27
A6NCG2	Solute carrier family 22 member 11	6.13	52.58
D6RGF0	Protein Largen	6.12	15.22
B0I1S4	DNHD1 variant protein	6.08	428.42
Q8IWQ8	SCAMPER	6.07	12.41
Q5TIG5	Afadin	6.05	189.04
Q05BX6	RABEP1 protein	6.04	82.33
Q8N3K9	Cardiomyopathy-associated protein 5	6.02	448.94
A0A024RDF7	Uncharacterized protein	5.99	130.17
O00757	Fructose-1,6-bisphosphatase isozyme 2	5.98	36.72
H0YC63	Microtubule-associated tumor suppressor 1	5.94	55.14
I3L3K8	Sodium-independent sulfate anion transporter	5.89	7.91
Q9HBD1	Roquin-2	5.88	131.59
B3KUX0	cDNA FLJ40831 fis, clone TRACH2012138	5.88	35.87
Q5JR59	Microtubule-associated tumor suppressor candidate 2	5.84	150.10
P26378	ELAV-like protein 4	5.84	41.74
C1KEQ3	GLCCI1	5.80	3.59
B2RWP0	Signal-induced proliferation-associated 1 like 3	5.80	194.50
A0A0A0MRJ3	Neuron navigator 1	5.80	197.28
Q8IXV0	HES1 protein	5.79	29.25

Accession Number	Description (protein name)		
A1L0S8	CROCC protein	5.79	129.39
Q5T1R4	Transcription factor HIVEP3	5.75	259.30
B2RE19	cDNA, FLJ96877	5.75	70.92
B4DSW4	cDNA FLJ51541, moderately similar to Transcription factor Sp8	5.69	16.42
Q6ZMY0	cDNA FLJ16598 fis, clone TESTI4006473, weakly similar to ATP-dependent RNA helicase A	5.67	150.88
C9JMI8	TBC1 domain family member 25	5.65	24.95
Q6UWX4	HHIP-like protein 2	5.02	80.73
A4PB67	YY1AP-related protein1	4.98	248.19
E9PG32	Dynein heavy chain 12, axonemal	4.97	454.03
Q6ZSX8	cDNA FLJ45139 fis, clone BRAWH3039623	4.92	15.46
O15078	Centrosomal protein of 290 kDa	4.91	290.21
Q8NDM7	Cilia- and flagella-associated protein 43	4.86	191.86
Q8N1H6	cDNA FLJ40869 fis, clone TSTOM2000139	4.79	53.78
O15014	Zinc finger protein 609	4.78	151.10
Q5TAX3	Terminal uridylyltransferase 4	4.31	185.05
B7Z7H2	cDNA FLJ58079, highly similar to Homo sapiens SH3 multiple domains 1 (SH3MD1), mRNA	4.04	106.32

CBMQ			
Accession Number	Description (protein name)	Ion count score	MW [kDa]
P04745	Alpha-amylase 1	606.56	57.73
F6KPG5	Albumin	166.66	66.49
P02814	Submaxillary gland androgen-regulated protein 3B	165.02	8.18
P06702	Protein S100-A9	160.46	13.23
Q6PJF2	IGK@ protein	137.04	25.50
C0JYZ2	Titin	129.49	3711.40
P01833	Polymeric immunoglobulin receptor	121.67	83.23
P01036	Cystatin-S	116.55	16.20
P01037	Cystatin-SN	95.10	16.38
A0A0C4DGN4	Zymogen granule protein 16 homolog B	88.79	19.59
P23280	Carbonic anhydrase 6	88.59	35.34
P25311	Zinc-alpha-2-glycoprotein	86.75	34.24
H6VRF8	Keratin 1	79.25	66.01
P12273	Prolactin-inducible protein	68.47	16.56
Q8WXI7	Mucin-16	60.58	1518.24
P0DOX7	Immunoglobulin kappa light chain	59.06	23.36
P05109	Protein S100-A8	56.20	10.83

P06733	Alpha-enolase	54.12	47.14
P01876	Immunoglobulin heavy constant alpha 1	50.62	37.63
E7ER44	Lactotransferrin	50.07	77.92
F5GZK2	Collagen alpha-1(XXI) chain	49.95	99.23
A0M8Q6	Immunoglobulin lambda constant 7	45.56	11.25
P04080	Cystatin-B	44.73	11.13
B4DW52	cDNA FLJ55253, highly similar to Actin, cytoplasmic 1	43.69	38.61
P13645	Keratin, type I cytoskeletal 10	41.19	58.79
B1AN48	Small proline-rich protein 3	39.34	16.95
P28325	Cystatin-D	38.76	16.07
A0A0A0MQW7	Leukocyte immunoglobulin-like receptor subfamily B member 4	38.27	14.44
Q0QET7	Glyceraldehyde-3-phosphate dehydrogenase	37.96	24.60
J3KNQ2	Fibronectin type III domain-containing protein 1	36.62	194.42
K7ESB7	Dedicator of cytokinesis protein 6	34.95	148.70
Q92954	Proteoglycan 4	33.41	150.98
G3V1A4	Cofilin 1 (Non-muscle), isoform CRA_a	33.14	16.80
E9PCT1	Serine/arginine repetitive matrix protein 1	25.61	93.38
A8K781	cDNA FLJ75299, highly similar to Xenopus laevis proteasome (prosome, macropain) 26S subunit, ATPase 3, mRNA	22.25	47.29
P31025	Lipocalin-1	21.55	19.24
Q7Z351	Putative uncharacterized protein DKFZp686N02209	20.15	52.82
V9HWC6	Peptidyl-prolyl cis-trans isomerase	19.72	22.73
Q1RMC9	ERBB2IP protein	19.23	153.42
A8K2I0	cDNA FLJ78504, highly similar to Homo sapiens keratin 6A (KRT6A), mRNA	18.91	59.99
A0A0J9YYJ7	Unconventional myosin-XVB	18.26	79.47
Q8WXG9	G-protein coupled receptor 98	17.79	692.64
B7Z830	cDNA FLJ61741, highly similar to HIRA protein	17.13	63.97
A0A087X1X8	Uncharacterized protein	17.12	21.74
B4E1B2	cDNA FLJ53691, highly similar to Serotransferrin	16.95	74.78
H7C517	Adenylate kinase 9	16.94	87.28
A0A087WW06	Tetratricopeptide repeat protein 28	16.70	256.71
C9JFF0	Kinesin-like protein KIF26A	16.48	180.04
Q59FL8	Receptor protein-tyrosine kinase	16.08	119.87
I0B0K8	Truncated profilaggrin	15.94	430.16
Q7Z5P9	Mucin-19	15.85	804.77
Q8WYP5	Protein ELYS	15.45	252.34
E1A689	Mutant Apo B 100	15.11	489.51

A0A0G2JRN3	Alpha-1-antitrypsin	14.72	40.21
E9PAV3	Nascent polypeptide-associated complex subunit alpha, muscle-specific for	14.61	205.29
P35527	Keratin, type I cytoskeletal 9	14.55	62.03
Q8TEA3	cDNA FLJ23738 fis, clone HEP15081, highly similar to PDZ domain-containing guanine nucleotide exchange factor I	14.54	126.03
B4E223	cDNA FLJ52075, moderately similar to Mus musculus SPT2, Suppressor of Ty, domain containing 1, mRNA	14.21	68.46
Q8N4F0	BPI fold-containing family B member 2	14.16	49.14
P49639	Homeobox protein Hox-A1	14.01	36.62
E7EVA0	Microtubule-associated protein	13.84	245.29
H9KV90	SH3 and multiple ankyrin repeat domains protein 1	13.51	225.76
T1S9D5	MUC5AC	13.45	521.30
Q8IVF2	Protein AHNAK2	13.23	616.24
Q86Y00	GTF2IRD2B protein	13.16	50.83
P10599	Thioredoxin	12.98	11.73
B7Z8H1	cDNA FLJ54814	12.92	24.15
B3KX86	cDNA FLJ44973 fis, clone BRAWH3001638	12.84	125.22
B2RNR6	Zinc finger RNA binding protein	12.52	116.94
B7ZLW1	CAMSAP1 protein	11.83	163.16
O15083	ERC protein 2	11.73	110.49
K7EJ44	Profilin	11.55	11.38
Q5CZC0	Fibrous sheath-interacting protein 2	11.49	780.12
Q5TAX3	Terminal uridylyltransferase 4	11.41	185.05
Q12830	Nucleosome-remodeling factor subunit BPTF	11.22	338.05
J3KPS2	Protein FAM83H	11.03	96.39
Q10571	Transcriptional activator MN1	10.98	135.92
H0Y9N7	Inhibitor of Bruton tyrosine kinase	10.90	14.09
Q5JPC9	ABI gene family, member 3 (NESH) binding protein, isoform CRA_d	10.38	110.61
H3BTR6	RNA-binding protein with serine-rich domain 1	10.27	12.99
A0A024QZH6	Serine arginine-rich pre-mRNA splicing factor SR-A1, isoform CRA_a	10.05	139.18
A4FUT8	JMJD1B protein	10.00	168.95
K7EL96	Perilipin-3	9.98	17.95
Q8TD20	Solute carrier family 2, facilitated glucose transporter member 12	9.93	66.92
A0A0G2JQF2	Formimidoyltransferase-cyclodeaminase	9.93	45.46
P54687	Branched-chain-amino-acid aminotransferase, cytosolic	9.86	42.94
B4DIS5	cDNA FLJ50076, highly similar to Liprin-alpha-4	9.84	103.07

Q9NR48	Histone-lysine N-methyltransferase ASH1L	9.81	332.58
P04275	von Willebrand factor	9.77	309.06
B4DUY9	cDNA FLJ56362	9.64	67.89
B4DHH1	cDNA FLJ57930, highly similar to Homo sapiens RAS guanyl releasing protein 1 (calcium and DAG-regulated) (RASGRP1), mRNA	9.42	85.17
A0A0C4DGV9	DNA ligase	9.19	96.15
B3KR01	cDNA FLJ33378 fis, clone BRACE2006354	8.90	46.07
J7M2B1	Tyrosine-protein kinase receptor	8.43	98.89
P25391	Laminin subunit alpha-1	8.36	336.87
Q5VST9	Obscurin	8.33	867.94
Q96L91	E1A-binding protein p400	8.04	343.28
Q8WXE0	Caskin-2	8.03	126.71
Q5T112	tRNA (adenine(37)-N6)-methyltransferase	7.96	17.35
A4PB67	YY1AP-related protein1	7.72	248.19
P80511	Protein S100-A12	7.56	10.57
Q6ZQQ6	WD repeat-containing protein 87	7.54	332.97
U3KPZ7	Uncharacterized protein	7.54	114.47
A7MBM6	MLL3 protein	7.40	362.42
A0A0A0MRS7	Ankyrin repeat and SAM domain-containing protein 6	7.10	62.27
J3KRI5	Cadherin-8	7.06	82.70
J3KQ96	Treacle protein	7.04	144.04
B2RMV2	CYTSA protein	6.98	124.50
D6RHX1	Mucin-7	6.94	15.45
B4E1M1	cDNA FLJ60391	6.86	73.88
F5GX59	Zonadhesin	6.84	282.23
H0Y6B5	Abl interactor 2	6.83	31.86
Q9Y608	Leucine-rich repeat flightless-interacting protein 2	6.82	82.12
E9PIQ4	Mth938 domain-containing protein	6.82	9.98
E9PPH6	Exophilin-5	6.77	192.96
Q9Y4D8	Probable E3 ubiquitin-protein ligase HECTD4	6.75	439.07
Q4G0P3	Hydrocephalus-inducing protein homolog	6.69	575.53
E5RIQ7	Eyes absent homolog	6.63	23.33
Q16880	2-hydroxyacylsphingosine 1-beta-galactosyltransferase	6.63	61.40
E9PCK9	Muscular LMNA-interacting protein	6.62	59.08
Q9P0X4	Voltage-dependent T-type calcium channel subunit alpha-1I	6.61	244.95
K7N7B3	Synaptonemal complex protein 2-like	6.59	93.44
Q6ZP01	RNA-binding protein 44	6.53	117.91
Q09666	Neuroblast differentiation-associated protein AHNAK	6.51	628.70

B3KY59	cDNA FLJ46903 fis, clone MESAN2003661, highly similar to Cdc42 effector protein 3 (Binder of Rho GTPases 2)	6.50	27.63
A8K5B3	cDNA FLJ76829, highly similar to Homo sapiens piggyBac transposable element derived 1 (PGBD1), mRNA	6.46	92.39
Q9BXW9	Fanconi anemia group D2 protein	6.44	164.02
H9NIL3	G protein-coupled receptor 20	6.42	38.64
G3V207	Transmembrane and coiled-coil domain family 3, isoform CRA_c	6.35	50.14
B4E2E5	cDNA FLJ56289, highly similar to Homo sapiens sperm specific antigen 2 (SSFA2), mRNA	6.34	119.13
Q96N67	Dedicator of cytokinesis protein 7	6.31	242.41
E9PNY3	Serine/threonine-protein phosphatase 2A 56 kDa regulatory subunit beta isoform	6.31	21.89
H0Y5R1	Aryl hydrocarbon receptor nuclear translocator-like protein 2	6.30	65.63
A0A0A0MQR4	Protein capicua homolog	6.29	163.58
Q9NTI5	Sister chromatid cohesion protein PDS5 homolog B	6.17	164.56
Q96BY6	Dedicator of cytokinesis protein 10	6.10	249.37
A0A140VJG7	Component of oligomeric golgi complex 6, isoform CRA_a	5.88	68.37
Q9NPV6	Putative uncharacterized protein DKFZp762E1511	5.86	17.77
Q8N8K9	Uncharacterized protein KIAA1958	5.75	79.16
J3QT10	N-lysine methyltransferase SETD6	5.67	45.57
Q9C0G0	Zinc finger protein 407	5.47	247.21
A0A0A0MRY1	Structural maintenance of chromosomes protein 6	5.27	50.91
D6RG39	OCIA domain-containing protein 1	5.01	19.01
Q96RW7	Hemicentin-1	4.98	613.00
A7MD03	CCDC132 protein	4.98	110.28
Q8WVS4	WD repeat-containing protein 60	4.93	122.50
Q96HA1	Nuclear envelope pore membrane protein POM 121	4.86	127.64
H0Y4R5	Transmembrane protein 201	4.82	59.80
Q8NB66	Protein unc-13 homolog C	4.78	250.75
H0Y4C5	NGFI-A-binding protein 1	4.75	27.75
Q59GI4	Zinc finger, FYVE domain containing 9 isoform 3 variant	4.69	145.96
E7EX73	Eukaryotic translation initiation factor 4 gamma 1	4.63	158.55
Q9BTC0	Death-inducer obliterator 1	4.31	243.72
A6NNC1	Putative POM121-like protein 1-like	4.14	94.00
DMQ			

Accession Number	Description (protein name)	Ion count score	MW [kDa]
Q8WXI7	Mucin-16	82.02	1518.2
P15515	Histatin-1	68.85	7.0
B7ZMD7	Alpha-amylase	66.23	57.7
D3DPG0	Titin, isoform CRA_a	65.09	3878.8
P02814	Submaxillary gland androgen-regulated protein 3B	61.25	8.2
Q7Z5P9	Mucin-19	50.38	804.8
B3KY63	cDNA FLJ16830 fis, clone UTERU3022536	43.22	215.1
F5GZK2	Collagen alpha-1(XXI) chain	37.05	99.2
P01036	Cystatin-S	33.12	16.2
A0A0U1RR20	Proteoglycan 4	30.51	146.4
Q86VQ1	Glucocorticoid-induced transcript 1 protein	29.92	58.0
E9PAV3	Nascent polypeptide-associated complex subunit alpha, muscle-specific form	24.97	205.3
Q5VST9	Obscurin	22.78	867.9
H0Y465	Neurofibromin	20.65	281.0
T1S9D5	MUC5AC	20.41	521.3
T1R7N3	MUC5AC	20.12	413.6
B4DH81	cDNA FLJ61250	19.95	93.5
B3KY54	cDNA FLJ46886 fis, clone UTERU3016308	19.84	61.6
Q5SYE7	NHS-like protein 1	19.49	170.6
Q9UQ35	Serine/arginine repetitive matrix protein 2	19.23	299.4
A7E2D6	NAV2 protein	18.74	261.6
F8W9J4	Dystonin	18.06	847.4
Q96Q06	Perilipin-4	18.01	134.3
J3KNQ2	Fibronectin type III domain-containing protein 1	17.88	194.4
Q15648	Mediator of RNA polymerase II transcription subunit 1	17.29	168.4
Q8N500	Putative uncharacterized protein	16.87	36.0
Q8IWQ1	TGS2	16.82	60.0
Q5T4S7	E3 ubiquitin-protein ligase UBR4	16.60	573.5
Q8IVF2	Protein AHNAK2	16.59	616.2
Q5VUA4	Zinc finger protein 318	16.47	251.0
I6L894	Ankyrin-2	16.31	430.0
Q03164	Histone-lysine N-methyltransferase 2A	16.13	431.5
Q13136	Liprin-alpha-1	15.76	135.7
Q8IVL0	Neuron navigator 3	15.67	255.5
B7ZA42	cDNA, FLJ79056	15.57	77.2

Q96HP0	Dedicator of cytokinesis protein 6	15.46	229.4
P25054	Adenomatous polyposis coli protein	14.87	311.5
A0A1B0GVP4	Ligand-dependent nuclear receptor corepressor-like protein	14.77	211.4
M0R2B3	Uncharacterized protein C19orf44	14.23	68.2
Q5D862	Filaggrin-2	14.14	247.9
O60307	Microtubule-associated serine/threonine-protein kinase 3	13.98	143.0
Q96F05	Uncharacterized protein C11orf24	13.94	46.1
C9JFF0	Kinesin-like protein KIF26A	13.74	180.0
Q9UKN1	Mucin-12	13.65	557.8
C9K0E4	Syntaxin-binding protein 5-like	13.62	111.2
O75592	E3 ubiquitin-protein ligase MYCBP2	13.48	509.8
L8E7G9	Alternative protein ZNF74	13.30	32.4
A6NK89	Ras association domain-containing protein 10	13.28	56.9
B7Z7S7	cDNA FLJ60964, weakly similar to Homo sapiens dentin sialophosphoprotein (DSPP), mRNA	13.27	37.7
B3KWI5	cDNA FLJ43124 fis, clone CTONG3004072, highly similar to Protein EMSY	13.26	130.7
E9PG32	Dynein heavy chain 12, axonemal	13.24	454.0
F5GYR0	Actin-binding LIM protein 2	13.13	71.3
H0YN99	Pseudopodium-enriched atypical kinase 1	13.13	115.1
Q9NR48	Histone-lysine N-methyltransferase ASH1L	13.06	332.6
Q9H5Y7	SLIT and NTRK-like protein 6	13.00	95.0
Q8TE73	Dynein heavy chain 5, axonemal	12.98	528.7
A7E2F7	CAP-GLY domain containing linker protein 2	12.95	111.7
Q5HYC2	Uncharacterized protein KIAA2026	12.85	227.9
A0A087WV20	Alstrom syndrome protein 1	12.77	425.0
Q5T1R4	Transcription factor HIVEP3	12.73	259.3
A7Y9J9	Mucin 5AC, oligomeric mucus/gel-forming	12.59	648.4
Q96RK0	Protein capicua homolog	12.58	163.7
A0A0J9YY01	Unconventional myosin-XVB	12.41	333.5
Q9Y2F5	Little elongation complex subunit 1	12.35	247.7
A0A087X1X8	Uncharacterized protein	12.31	21.7
A0A0A0MS59	Helicase SRCAP	12.23	315.4
A1L4H1	Soluble scavenger receptor cysteine-rich domain-containing protein SSC5D	12.20	165.6
H7BZX1	Sorbin and SH3 domain-containing protein 2	12.05	27.5
S6C4Q9	IgG L chain	12.01	22.8
B4DWY3	cDNA FLJ56165, highly similar to RNA exonuclease 1 homolog (EC 3.1.-.-)	11.79	58.3
P54274	Telomeric repeat-binding factor	11.68	50.2

Q2TAZ0	Autophagy-related protein 2 homolog A	11.55	212.7
P78310	Coxsackievirus and adenovirus receptor	11.50	40.0
A6NM62	Leucine-rich repeat-containing protein 53	11.39	140.7
Q96LR2	Leucine rich adaptor protein 1	11.24	25.8
K9N2R0	Interleukin 15 receptor alpha isoform IC8 OS=Ho	11.14	30.8
Q9H2L7	DC33	11.06	29.5
Q9UHB7	AF4/FMR2 family member 4	10.92	127.4
Q92766	Ras-responsive element-binding protein 1	10.85	181.3
Q59GL0	Rearranged L-myc fusion sequence variant	10.64	184.6
Q7Z4S6	Kinesin-like protein KIF21A	10.60	187.1
Q6GMQ3	PHC1 protein	10.56	100.1
Q6KC79	Nipped-B-like protein	10.53	315.9
A0A087WVZ6	Protein kinase C-binding protein 1	10.51	125.7
A0A087WXN4	Integrator complex subunit 12	10.51	46.6
Q6ZU65	Ubinuclein-2	10.41	146.0
E7EWQ5	Microtubule-associated serine/threonine-protein kinase 4	10.40	266.0
A0A075B756	Krueppel-like factor 14	10.39	33.1
F1T0K4	DmX-like protein 1	10.38	318.4
H3BTR6	RNA-binding protein with serine-rich domain 1	10.36	13.0
Q2M2I8	AP2-associated protein kinase 1	10.28	103.8
Q9BXF6	Rab11 family-interacting protein 5	10.26	70.4
A8KAL3	cDNA FLJ77478, highly similar to Homo sapiens Rho GTPase activating protein 6 (ARHGAP6), transcript variant 1, mRNA	10.24	105.8
P78409	Butyrophilin	10.20	81.3
H7C1I7	Zinc finger MYM-type protein 4	10.19	134.3
Q15772	Striated muscle preferentially expressed protein kinase	10.18	354.1
A8K5H6	cDNA FLJ76659, highly similar to Homo sapiens exonuclease 1 (EXO1), transcript variant 2, mRNA	10.14	93.8
H0YKJ2	Solute carrier family 12 member 6	10.12	14.8
A0A024QZH6	Serine arginine-rich pre-mRNA splicing factor SR-A1, isoform CRA_a	10.11	139.2
Q5T088	MORN repeat-containing protein 1	10.02	19.7
A0A1W2PR28	IQ motif and SEC7 domain-containing protein 2	10.01	127.9
Q9H6K5	Proline-rich protein 36	9.98	132.7
Q5JW04	Solute carrier family 35 member C2	9.98	21.8
O95425	Supervillin	9.97	247.6
Q5JPC9	ABI gene family, member 3 (NESH) binding protein, isoform CRA_d	9.96	110.6
A0A1W2PRA7	Calcium-activated potassium channel subunit alpha-1	9.96	107.9

P16188	HLA class I histocompatibility antigen, A-30 alpha chain	9.96	40.9
P51826	AF4/FMR2 family member 3	9.93	133.4
A0A087WU78	Nance-Horan syndrome protein	9.93	157.7
B4E063	Kinesin-like protein	9.93	73.0
A0A024RDD6	Uncharacterized protein	9.87	82.4
Q5VWG9	Transcription initiation factor TFIID subunit 3	9.84	103.5
Q96JG9	Zinc finger protein 469	9.81	409.9
Q14690	Protein RRP5 homolog	9.78	208.6
Q8NFC6	Biorientation of chromosomes in cell division protein 1-like 1	9.78	330.3
O15457	MutS protein homolog 4	9.76	104.7
A0A024RB02	PTPRF interacting protein, binding protein 1 (Liprin beta 1), isoform CRA_a	9.75	96.9
B4DYH4	cDNA FLJ51571, moderately similar to Mediator of DNA damage checkpoint protein 1	9.75	178.6
Q5T7P2	Late cornified envelope protein 1A	9.71	11.0
A0A024R1T4	Trinucleotide repeat containing 6B, isoform CRA_b	9.71	162.1
Q9C0D5	Protein TANC1	9.68	202.1
A0A0A0MTR7	E3 ubiquitin-protein ligase RNF213	9.67	591.0
H0YLX2	DNA-binding protein RFX7	9.65	137.4
S4R418	Bridging integrator 2	9.63	59.0
Q9P206	Uncharacterized protein KIAA1522	9.61	107.0
Q14395	Mucin	9.59	51.9
B2RWP0	Signal-induced proliferation-associated 1 like 3	9.58	194.5
A2A2V2	RNA-binding protein 34	9.57	45.9
A8K119	cDNA FLJ76742, highly similar to Homo sapiens deleted in liver cancer 1 (DLC1), transcript variant 2, mRNA	9.55	122.7
X6R7H2	Peroxisome proliferator-activated receptor gamma coactivator-related protein 1	9.53	69.1
Q86UU5	Gametogenetin	9.53	66.7
Q8WY24	SNC66 protein	9.48	53.6
I0B0K6	Truncated profilaggrin	9.46	277.1
Q8N122	Regulatory-associated protein of mTOR	9.44	148.9
Q8NEY1	Neuron navigator 1	9.43	202.3
Q86YZ3	Hornerin	9.42	282.2
Q9C0B5	Palmitoyltransferase ZDHHC5	9.41	77.5
Q64FY1	AKNA transcript B1	9.38	146.2
E7EPM4	Mucin-17	9.38	425.3
B7ZKL5	AXIN2 protein	9.34	86.6
Q59FR9	Fibroblast growth factor 11 variant	9.23	36.4

A0A0A0MSP7	FERM and PDZ domain-containing protein 3	9.18	193.4
A0A024RDF7	Uncharacterized protein	9.17	130.2
Q8IZF6	Adhesion G-protein coupled receptor G4	9.17	333.2
H0Y785	Ankyrin repeat and KH domain-containing protein 1	9.14	107.8
B8XCX8	EPC1/ASXL2b fusion protein	9.12	201.7
A0A087WX12	Centrosomal protein kizuna	9.08	49.3
Q8IZT6	Abnormal spindle-like microcephaly-associated protein	9.07	409.5
Q5KU26	Collectin-12	9.06	81.5
P17948	Vascular endothelial growth factor receptor 1	8.97	150.7
B3KVI8	cDNA FLJ16604 fis, clone TESTI4008097	8.95	157.9
Q9Y6R7	IgGFc-binding protein	8.87	571.6
A0A140VJJ5	Testicular tissue protein Li 69	8.79	119.7
A8K8Q0	cDNA FLJ78753, highly similar to Homo sapiens zinc fingers and homeoboxes 3 (ZHX3), mRNA	8.76	104.6
L8E9Z3	Alternative protein HRC	8.45	34.3
A0A126LB25	Immediate early protein IE2	8.44	164.2
Q8IY33	MICAL-like protein 2	8.39	97.4
B3KR06	CLIP-associating protein 2	8.38	49.1
C9JG08	Uncharacterized protein C2orf16	8.19	598.1
Q9ULH0	Kinase D-interacting substrate of 220 kDa	8.15	196.4
E1A689	Mutant Apo B 100	8.09	489.5
Q12955	Ankyrin-3	7.98	480.1
Q53QN0	Putative uncharacterized protein GTF3C2	7.78	58.4
Q96BY7	Autophagy-related protein 2 homolog B	7.75	232.6
B0QYZ7	Eukaryotic translation initiation factor 4E transporter	7.56	26.0
Q20BI6	Cystic fibrosis transmembrane conductance regulator	7.50	150.1
Q96MW7	Tigger transposable element-derived protein 1	7.38	67.3
B3KWK5	cDNA FLJ43230 fis, clone HCHON2001269	7.36	24.2
E3W980	Helicase POLQ-like	7.34	116.7
Q45KX0	Brevideltin	7.33	22.1
Q8N2C7	Protein unc-80 homolog	7.28	363.2
B4DYX2	cDNA FLJ51404, highly similar to Netrin receptor DCC	7.27	99.0
F2Z2B6	Protein Jade-3	7.24	13.1
B4E2K8	cDNA FLJ61075, highly similar to Mineralocorticoid receptor	7.17	67.8
H0YMD1	Low-density lipoprotein receptor	7.14	104.7
O75132	Zinc finger BED domain-containing protein 4	7.12	130.2
H0YM61	Transient receptor potential cation channel subfamily M member 1	7.12	57.3

B4DWC0	cDNA FLJ58290, highly similar to Zinc finger MYM-type protein 6	7.09	96.9
B4DNH7	cDNA FLJ60079, highly similar to Tetratricopeptide repeat protein 3	7.09	99.7
E9PPY5	Mas-related G-protein-coupled receptor member X3	7.08	27.8
K7EKF7	Voltage-dependent P/Q-type calcium channel subunit alpha-1A	7.06	98.8
A0A0U1RQK2	Casein kinase I isoform gamma-1	7.03	15.4
H0UI11	Dopey family member 1, isoform CRA_a	7.02	255.6
A2NH55	Immunogobulin kappa, VJ region	7.00	11.9
Q8N7X0	Androglobin	6.99	189.6
Q6ZS54	cDNA FLJ45821 fis, clone NT2RP8001584	6.96	79.2
Q5T4T1	Transmembrane protein 170B	6.96	14.4
B4E0Q3	cDNA FLJ51432, highly similar to Dynamin-binding protein	6.96	57.9
A0A096LNL9	Transcriptional regulator ATRX	6.94	151.6
Q8N9U0	Tandem C2 domains nuclear protein	6.92	55.2
A0A087WW06	Tetratricopeptide repeat protein 28	6.92	256.7
F2Z357	Rap1 GTPase-activating protein 1	6.91	66.9
B4DMP4	cDNA FLJ53136, highly similar to Homo sapiens Vac14 homolog (VAC14), mRNA	6.91	80.1
A0A024R952	Plakophilin 1 (Ectodermal dysplasia/skin fragility syndrome), isoform CRA_a	6.91	80.4
B4DRA2	cDNA FLJ57828, highly similar to Treacle protein	6.89	93.7
A8K8T9	cDNA FLJ77187, highly similar to Homo sapiens cyclin B3 (CCNB3), transcript variant 3, mRNA	6.88	157.8
B3KX64	cDNA FLJ44873 fis, clone BRAMY2023939	6.87	77.9
D6RFH5	Folliculin-interacting protein 2	6.86	74.7
B3KV77	cDNA FLJ16222 fis, clone CTONG3002947	6.85	56.3
D6RBK6	Type-1 angiotensin II receptor-associated protein	6.85	16.4
A0A1B0GUW1	Phosphatidylinositol N-acetylglucosaminyltransferase subunit Q	6.85	6.9
B3KXH9	cDNA FLJ45423 fis, clone BRHIP3036936	6.84	110.1
H0YHI8	Protein phosphatase 1 regulatory subunit 12A	6.83	40.6
B4DG67	cDNA FLJ58842, highly similar to Homo sapiens zinc and ring finger 1 (ZNRF1), mRNA	6.83	21.8
Q5SWA1	Protein phosphatase 1 regulatory subunit 15B	6.82	79.1
B4DLG2	cDNA FLJ58196, highly similar to Zinc finger CCCH domain-containing protein 11A	6.81	82.7
Q6ZVL6	UPF0606 protein KIAA1549L	6.81	198.9
Q6WRX3	Protein zyg-11 homolog A	6.79	85.8
Q59FL0	Misshapen/NIK-related kinase isoform 2 variant	6.78	93.2

D3DTH7	Myosin IC, isoform CRA_a	6.77	98.9
Q9HBR1	Putative uncharacterized protein	6.77	50.4
Q71F56	Mediator of RNA polymerase II transcription subunit 13-like	6.77	242.4
C9J0I9	Nuclear-interacting partner of ALK	6.76	50.5
Q8N237	cDNA FLJ34965 fis, clone NTONG2004308	6.76	99.0
A0A024RD26	G protein-coupled receptor 116, isoform CRA_a	6.75	149.3
S4R3C2	Nucleolar and coiled-body phosphoprotein 1	6.75	29.3
A0A1W2PPB5	Bone morphogenetic protein receptor type-2	6.74	57.0
C9JJU3	Bromodomain testis-specific protein	6.74	52.8
A0A0C4DFX2	Protein furry homolog	6.74	338.0
Q7Z408	CUB and sushi domain-containing protein 2	6.73	379.8
G3V1X1	Proline/serine-rich coiled-coil 2, isoform CRA_a	6.72	39.1
Q68D69	Putative uncharacterized protein DKFZp779G1236	6.72	113.3
Q9BU23	Lipase maturation factor 2	6.71	79.6
B2RMV2	CYTSA protein	6.71	124.5
P08217	Chymotrypsin-like elastase family member 2A	6.71	28.9
Q5VV42	Threonylcarbamoyladenosine tRNA methylthiotransferase	6.69	65.1
E7EX48	Serine/threonine-protein kinase Nek4	6.69	80.6
E9PL24	Myomegalin	6.69	126.9
Q9C0D2	Centrosomal protein of 295 kDa	6.68	295.0
A8KAE4	cDNA FLJ75520	6.68	131.2
C9JN15	Peptidyl-prolyl cis-trans isomerase	6.67	27.4
C9JG84	Sorbin and SH3 domain-containing protein 2	6.67	12.3
Q5JPB2	Zinc finger protein 831	6.66	177.8
Q6NUQ2	Calmin (Calponin-like, transmembrane)	6.66	111.6
Q9ULL8	Protein Shroom4	6.65	164.8
H0YBF7	Arf-GAP with SH3 domain, ANK repeat and PH domain-containing protein 1	6.65	105.2
H9KVB3	Otogelin	6.64	313.2
A2RQD7	Bcr-abl1 e19a2 chimeric protein	6.64	56.6
P55291	Cadherin-15	6.64	88.9
Q53H75	Chromosome 14 open reading frame 133 variant	6.63	57.0
B4DL51	cDNA FLJ60657, highly similar to Homo sapiens Smith-Magenis syndrome chromosome region, candidate 8 (SMCR8), mRNA	6.63	75.3
H3BU24	S phase cyclin A-associated protein in the endoplasmic reticulum	6.63	6.4
E9PML0	Cytochrome P450 4B1	6.62	36.4
A5PLN7	Protein FAM149A	6.61	82.6

Q59G99	Dishevelled 1 isoform a variant	6.61	40.3
A0A140T8X5	STK19	6.61	40.4
B2R621	cDNA, FLJ92736, highly similar to Homo sapiens gamma-aminobutyric acid (GABA) A receptor, alpha 3 (GABRA3), mRNA	6.60	55.1
A6NJB7	Proline-rich protein 19	6.60	38.7
L8E8M9	Alternative protein PCDHB16	6.60	9.1
B3KU03	cDNA FLJ39022 fis, clone NT2RP7003724	6.60	64.6
Q9HCK8	Chromodomain-helicase-DNA-binding protein 8	6.59	290.3
Q8IYW4	ENTH domain-containing protein 1	6.57	67.5
Q2VIN3	RBM1	6.57	41.4
B7ZKN6	UTX protein	6.54	149.2
F8WAI8	Zinc finger and BTB domain-containing protein 40	6.53	125.4
Q13489	Baculoviral IAP repeat-containing protein 3	6.52	68.3
H0Y482	Band 4.1-like protein 1	6.52	13.0
Q53FJ3	Ubiquitin specific protease, proto-oncogene isoform a variant	6.52	108.5
Q7Z540	Mucin short variant SV7	6.50	13.4
E9PNK1	Sialidase-3	6.50	18.8
H0YGG9	Solute carrier organic anion transporter family member	6.49	52.7
Q5M9N0	Coiled-coil domain-containing protein 158	6.48	127.1
D6RFZ4	Protein FAM193A	6.48	87.2
Q9P2Q4	5-hydroxytryptamine (Serotonin) receptor 1F	6.48	41.6
Q68DX6	Putative uncharacterized protein DKFZp686P0776	6.46	78.0
B0QZ65	GTPase-activating protein and VPS9 domain-containing protein 1	6.45	56.4
B4DX00	cDNA FLJ61440, highly similar to Izumo sperm-egg fusion protein 1	6.45	26.4
Q9Y6R1	Electrogenic sodium bicarbonate cotransporter 1	6.45	121.4
Q96GX5	Serine/threonine-protein kinase greatwall	6.44	97.3
B4E124	Ankyrin repeat and LEM domain-containing protein 1	6.43	46.6
B4DR76	cDNA FLJ58249, highly similar to Eukaryotic translation initiation factor 4E transporter	6.43	68.9
A8K482	Aspartate aminotransferase	6.43	47.5
Q8IY92	Structure-specific endonuclease subunit SLX4	6.43	199.9
Q7Z2Z1	Treslin	6.43	210.7
Q8N397	Putative uncharacterized protein DKFZp761M142	6.42	89.8
Q9H195	Mucin-3B	6.42	131.3
B3KUT9	cDNA FLJ40599 fis, clone THYMU2011183, highly similar to Thymus-specific serine protease (EC3.4.-.-)	6.41	27.5
A7MD48	Serine/arginine repetitive matrix protein 4	6.41	68.5

A0A1B0GTR8	Ankyrin repeat and fibronectin type-III domain-containing protein 1	6.40	56.4
B7Z5R7	cDNA FLJ61355, highly similar to CLIP-associating protein 1	6.40	135.7
Q8IX28	SE2-5LT1 protein	6.39	89.6
O43147	Small G protein signaling modulator 2	6.39	113.2
B4DNH6	Perilipin	6.39	38.4
F8VY01	FYVE, RhoGEF and PH domain-containing protein 6	6.39	135.4
B2RU27	Testis expressed 15	6.38	315.1
Q9ULK2	Ataxin-7-like protein 1	6.38	91.5
A0A1W2PQT4	KAT8 regulatory NSL complex subunit 1	6.38	58.4
A6ND36	Protein FAM83G	6.36	90.8
Q8N4A7	Putative uncharacterized protein	6.36	8.0
Q9BX26	Synaptonemal complex protein 2	6.35	175.5
H0YCA1	Plasma protease C1 inhibitor	6.34	9.9
B3KS23	cDNA FLJ35336 fis, clone PROST2015464	6.34	56.4
A0A1S5UZH2	Protein-methionine sulfoxide oxidase	6.34	116.8
G0Z071	Sex-determining region Y protein	6.33	23.8
L8E9J7	Alternative protein GPR78	6.33	9.6
B5MCY1	Tudor domain-containing protein 15	6.32	221.6
H0YAA7	Endomucin	6.32	8.0
Q8WYX5	Putative uncharacterized protein pp10472	6.31	17.9
I3L209	Transforming growth factor beta-1-induced transcript 1 protein	6.31	6.5
Q53TA0	Receptor protein-tyrosine kinase	6.30	79.0
H7BXS9	Trinucleotide repeat-containing gene 18 protein	6.29	42.6
H0Y5R1	Aryl hydrocarbon receptor nuclear translocator-like protein 2	6.29	65.6
Q9BRL6	Serine/arginine-rich splicing factor 8	6.23	32.3
Q96KW2	POM121-like protein 2	6.23	109.8
H0Y7V4	Dynein heavy chain 8, axonemal	6.23	478.6
A0A075B7B7	GAS2-like protein 2	6.19	94.8
B6RC65	Epidermal growth factor receptor variant EX12_14del	6.18	15.0
B4DDG9	cDNA FLJ53856, highly similar to 5-aminolevulinate synthase, nonspecific, mitochondrial (EC 2.3.1.37)	6.17	48.8
Q684P5	Rap1 GTPase-activating protein 2	6.16	80.0
Q9UBL0	cAMP-regulated phosphoprotein 21	6.15	89.1
Q9BW04	Specifically androgen-regulated gene protein	6.15	63.9
A0A0G2JN42	Mucin-6	6.14	256.9
Q2XPN4	Mitochondrial A kinase PPKA anchor protein 10	6.08	67.7

Q9UND0	Killer inhibitory receptor 2-2-1	6.06	14.3
E7EU81	Golgin subfamily B member 1	6.05	188.1
H0UIC5	Ecotropic viral integration site 2B, isoform CRA_a	6.04	39.9
B4E1T1	cDNA FLJ54081, highly similar to Keratin, type II cytoskeletal 5	6.04	58.8
P46013	Proliferation marker protein Ki-67	6.04	358.5
O43419	Intestinal mucin	6.02	60.5
Q9NWN3	F-box only protein 34	6.02	78.7
A0A024R8E8	Senataxin, isoform CRA_b	6.01	199.9
B7Z5J1	cDNA FLJ59265, highly similar to NAD-dependent deacetylase sirtuin-3, mitochondrial (EC 3.5.1.-)	6.01	37.6
B3KME0	cDNA FLJ10760 fis, clone NT2RP3004618	6.01	88.7
Q59FF8	CUB and Sushi multiple domains 1 variant	6.00	323.3
A0A024R3H2	Sortilin-related receptor, L(DLR class) A repeats-containing, isoform CRA_b	5.98	248.3
E9PHY1	Low-density lipoprotein receptor-related protein 5	5.96	52.4
C9JT44	Solute carrier family 25 member 38	5.95	16.6
B3KR17	cDNA FLJ33465 fis, clone BRAMY2001367	5.94	86.5
Q6ZR29	cDNA FLJ46702 fis, clone TRACH3014183	5.91	160.1
D6RDI1	E3 ubiquitin-protein ligase MIB2	5.90	11.6
Q05DV5	ZC3HAV1 protein	5.90	49.2
B4DS83	cDNA FLJ53179, highly similar to Nucleolar protein 10	5.88	74.4
D2CPJ9	Mutant mutant xeroderma pigmentosum complementation group C protein	5.84	25.7
Q6ZU64	Cilia- and flagella-associated protein 65	5.83	217.1
B2R8T0	cDNA, FLJ94049, highly similar to Homo sapiens egf-like module containing, mucin-like, hormonereceptor-like sequence 1 (EMR1), mRNA	5.82	97.7
A8K857	cDNA FLJ76361	5.82	23.5
B7Z7H2	cDNA FLJ58079, highly similar to Homo sapiens SH3 multiple domains 1 (SH3MD1), mRNA	5.81	106.3
P0C7P2	Putative protein RFPL3S	5.81	11.7
H0YLM8	DmX-like protein 2	5.80	132.6
B4DG65	cDNA FLJ52105, highly similar to PDZ domain-containing RING finger protein 4	5.79	89.0
K4DI93	Cullin 4B, isoform CRA_e	5.71	102.7
A8K601	cDNA FLJ75186	5.70	118.4
B7Z3E3	Reticulon	5.69	100.8
P27815	cAMP-specific 3',5'-cyclic phosphodiesterase 4A	5.69	98.1
A0A1B0GTP3	Long intergenic non-protein coding RNA 238	5.64	18.9

Q86U11	Full-length cDNA clone CS0DE006YM09 of Placenta of Homo sapiens (human)	5.47	47.7
A0A0B4J2E9	High affinity immunoglobulin epsilon receptor subunit beta	5.30	21.6
K7EIU2	Serine/threonine-protein kinase ULK2	5.26	21.0
B2R7I0	cDNA, FLJ93451, highly similar to Homo sapiens thioredoxin domain containing 14 (TXNDC14), mRNA	5.23	34.0
Q5VSN0	SH3 domain-containing kinase-binding protein 1	5.22	61.4
A0A087WVA8	Testis-expressed protein 2	5.22	125.3
F8WF20	Integrin beta-1-binding protein 1	5.21	4.3
F5GYN0	Protein FAM186A	5.09	262.1
B3KN94	cDNA FLJ13982 fis, clone Y79AA1001711	5.05	62.0
E9PBD8	Lymphocyte-specific protein 1	4.85	24.4
Q59EZ3	Insulin-like growth factor 2 receptor variant	4.69	265.9

Table 3. Overlapping pellicle proteins present on metallic brackets surface (BMQ), ceramic brackets (CBMQ) and HA discs (DMQ)

BMQ/CBMQ/DMQ	Accession Number	Description (protein name)	Peptides Identification	MW [kDa]	calc. pI
Total: 9	P02814	Submaxillary gland androgen-regulated protein 3B	2	8.2	9.57
	F5GZK2	Collagen alpha-1(XXI)	3	99.2	8.47
	Q8WXI7	Mucin-16	14	1518.2	5.26
	E9PAV3	Nascent polypeptide-associated complex subunit alpha	6	205.3	9.58
	Q7Z5P9	Mucin-19	7	804.8	5.01
	Q5VST9	Obscurin	3	867.9	5.99
	Q9NR48	Histone-lysine N-methyltransferase ASH1L	3	332.6	9.39
	Q8IVF2	Protein AHNAK2	3	616.2	5.36
	C9JFF0	Kinesin-like protein KIF26A	2	180	8.9

BMQ/CBMQ	Accession Number	Description (protein name)	Peptides Identification	MW [kDa]	calc. pI
Total: 18	P13645	Keratin, type I cytoskeletal 10	13	58.8	5.21
	H6VRF8	Keratin 1	13	66	8.12
	P35527	Keratin, type I cytoskeletal 9	7	62	5.24
	Q92954	Proteoglycan 4	3	151	9.5
	Q5CZC0	Fibrous sheath-interacting protein 2	7	780.1	6.71
	A0A0J9YYJ7	Unconventional myosin-XVB	3	79.5	9.61
	A8K781	cDNA FLJ75299	3	47.3	5.22
	Q8WXG9	G-protein coupled receptor 98	4	692.6	4.64
	Q96HA1	Nuclear envelope pore membrane protein POM 121	2	127.6	10.56
	J3KQ96	Treacle protein	3	144	8.29
	B7ZLW1	CAMSAP1 protein	3	163.2	6.95
	I0B0K8	Truncated profilaggrin	3	430.2	9.29
	Q8WVS4	WD repeat-containing protein 60	3	122.5	7.31
	Q8NB66	Protein unc-13 homolog C	3	250.8	5.92
	B4E223	cDNA FLJ52075	2	68.5	9.85

	Accession Number	Description (protein name)	Peptides Identification	MW [kDa]	calc. pI
	F5GX59	Zonadhesin	2	282.2	5.96
	A4PB67	YY1AP-related protein1	2	248.2	5.01
	Q5TAX3	Terminal uridylyltransferase 4	2	185	7.97

BMQ/CBMQ	Accession Number	Description (protein name)	Peptides Identification	MW [kDa]	calc. pI
Total: 36	P15515	Histatin-1	2	7	9.14
	A2A2V2	RNA-binding protein 34	2	45.9	10.08
	T1R7N3	MUC5AC	4	413.6	8.09
	Q5SYE7	NHS-like protein 1	4	170.6	6.96
	Q86YZ3	Hornerin	4	282.2	10.04
	B8XCX8	EPC1/ASXL2b fusion protein	5	201.7	8.53
	B4DH81	cDNA FLJ61250	2	93.5	6.92
	P51826	AF4/FMR2 family member 3	3	133.4	8.1
	Q8IVL0	Neuron navigator 3	4	255.5	8.76
	Q6ZU65	Ubinuclein-2	3	146	9.19
	O75592	E3 ubiquitin-protein ligase MYCBP2	4	509.8	7.03
	A0A1W2PR28	IQ motif and SEC7 domain-containing protein 2	3	127.9	6.96
	Q96JG9	Zinc finger protein 469	3	409.9	7.72
	Q5T4S7	E3 ubiquitin-protein ligase UBR4	3	573.5	6.04
	X6R7H2	Peroxisome proliferator-activated receptor gamma coactivator-related protein 1	3	69.1	10.04
	Q96F05	Uncharacterized protein C11orf24	2	46.1	5.87
	Q59G99	Dishevelled 1 isoform a variant	2	40.3	8.24
	E7EPM4	Mucin-17	3	425.3	4.03
	P46013	Proliferation marker protein Ki-67	3	358.5	9.45
	Q9HCK8	Chromodomain-helicase-DNA-binding protein 8	2	290.3	6.47
	Q5VWG9	Transcription initiation factor TFIID subunit 3	3	103.5	9.06
	P25054	Adenomatous polyposis coli protein	3	311.5	7.8

	Accession Number	Description (protein name)	Peptides Identification	MW [kDa]	calc. pI
	A0A140VJJ5	Testicular tissue protein Li 69	2	119.7	9.39
	Q9UKN1	Mucin-12	2	557.8	5.55
	O60307	Microtubule-associated serine/threonine-protein kinase 3	2	143	8.06
	E9PL24	Myomegalin	2	126.9	5.27
	Q96KW2	POM121-like protein 2	2	109.8	9.89
	L8E9Z3	Alternative protein HRC	2	34.3	11.99
	Q9C0D2	Centrosomal protein of 295 kDa	2	295	6
	B2RWP0	Signal-induced proliferation-associated 1 like 3	2	194.5	8.32
	A0A024RDF7	Uncharacterized protein	2	194.5	7.8
	Q5T1R4	Transcription factor HIVEP3	2	259.3	7.81
	B7Z7H2	cDNA FLJ58079	2	106.3	8.44
CBMQ/DMQ	Accession Number	Description (protein name)	Peptides Identification	MW [kDa]	calc. pI
Total: 11	H0Y5R1	Aryl hydrocarbon receptor nuclear translocator-like protein 2	2	65.6	7.8
	Q5JPC9	ABI gene family, member 3 (NESH) binding protein, isoform CRA_d	3	110.6	10.1
	E1A689	Mutant Apo B 100	2	489.5	7.1
	H3BTR6	RNA-binding protein with serine-rich domain 1	3	12.9	11.2
	B2RMV2	CYTSA protein	2	124.5	5.7
	A0A024QZH6	Serine arginine-rich pre-mRNA splicing factor SR-A1, isoform CRA_a	3	139.1	9.2
	A0A024RDD6	Uncharacterized protein	3	82.3	7.5
	A0A087WW06	Tetratricopeptide repeat protein 28	2	256.7	6.8
	T1R7N3	MUC5AC	6	413.6	8
	J3KNQ2	Fibronectin type III domain-containing protein 1	6	194.4	9.2
	P01036	Cystatin-S	3	16.2	5

Table 4. The Twenty more abundant proteins present in each group (metallic brackets surface (BMQ), ceramic brackets (CBMQ) and HA discs (DMQ)) with their respective pI

BMQ	Accession Number	Description (protein name)	Ion count score	Coverage	Peptides Identification	MW [kDa]	calc. pI
20 of 298 found	P13645	Keratin, type I cytoskeletal 10	263.77	33.90	13	58.8	5.21
	A0A0A0MTS7	Titin	175.26	1.26	25	3992.2	6.39
	H6VRF8	Keratin 1	175.13	27.48	13	66.0	8.12
	P02814	Submaxillary gland androgen-regulated protein 3B	105.99	65.82	2	8.2	9.57
	P35527	Keratin, type I cytoskeletal 9	96.87	25.84	7	62.0	5.24
	P35908	Keratin, type II cytoskeletal 2 epidermal	96.10	45.23	14	65.4	8.00
	M0R088	Serine/arginine repetitive matrix protein 1	59.52	6.75	5	78.1	12.06
	Q6ZRI6	Uncharacterized protein C15orf39	56.38	4.49	2	110.6	7.64
	P15515	Histatin-1	54.31	36.84	2	7.0	9.13
	B3KXW2	cDNA FLJ46178 fis, clone TESTI4003944	50.78	4.15	3	141.6	8.65
	F5GZK2	Collagen alpha-1(XXI)	49.95	3.77	3	99.2	8.47
	Q8WXI7	Mucin-16	47.89	2.55	14	1518.2	5.26
	Q96RT6	cTAGE family member 2	41.43	4.97	2	85.2	6.16
	B4DRU6	cDNA FLJ54657, highly similar to Keratin, type II cytoskeletal 6A	39.88	12.39	5	58.5	7.37
	Q92954	Proteoglycan 4	39.63	4.42	3	151.0	9.50
	Q5CZC0	Fibrous sheath-interacting protein 2	34.44	2.01	7	780.1	6.71
	B4DVQ0	cDNA FLJ58286, highly similar to Actin, cytoplasmic 2	33.09	13.51	3	37.3	5.71

	A0A0J9YYJ7	Unconventional myosin-XVB	32.86	9.47	3	79.5	9.61
	A2A2V2	RNA-binding protein 34	32.18	3.68	2	45.9	10.08
	B3KNX8	cDNA FLJ30689 fis, clone FCBBF2000566	30.34	10.65	3	84.5	6.28
CBMQ	Accession Number	Description (protein name)	Ion count score	Coverage	Peptides Identification	MW [kDa]	calc. pI
20 of 154 found	P04745	Alpha-amylase 1	606.56	57.34	21	57.7	6.93
	F6KPG5	Albumin	166.66	18.63	11	66.5	6.04
	P02814	Submaxillary gland androgen-regulated protein 3B	165.02	65.82	2	8.2	9.57
	P06702	Protein S100-A9	160.46	73.68	7	13.2	6.13
	Q6PJF2	IGK@ protein	137.04	29.36	6	25.5	6.55
	C0JYZ2	Titin	129.49	0.77	13	3711.4	6.52
	P01833	Polymeric immunoglobulin receptor	121.67	16.23	9	83.2	5.74
	P01036	Cystatin-S	116.55	53.19	6	16.2	5.02
	P01037	Cystatin-SN	95.10	56.74	6	16.4	7.21
	A0A0C4DGN4	Zymogen granule protein 16 homolog B	88.79	43.26	4	19.6	5.95
	P23280	Carbonic anhydrase 6	88.59	25.00	5	35.3	7.02
	P25311	Zinc-alpha-2-glycoprotein	86.75	28.19	5	34.2	6.05
	H6VRF8	Keratin 1	79.25	17.24	8	66.0	8.12
	P12273	Prolactin-inducible protein	68.47	26.03	4	16.6	8.05
	Q8WXI7	Mucin-16	60.58	3.41	18	1518.2	5.26
	P0DOX7	Immunoglobulin kappa light chain	59.06	33.18	5	23.4	7.17
	P05109	Protein S100-A8	56.20	38.71	4	10.8	7.03
	P06733	Alpha-enolase	54.12	30.88	7	47.1	7.39
	P01876	Immunoglobulin heavy constant alpha 1	50.62	20.96	4	37.6	6.51
	E7ER44	Lactotransferrin	50.07	13.14	5	77.9	8.12

DMQ	Accession Number	Description (protein name)	Ion count score	Coverage	Peptides Identification	MW [kDa]	calc. pI
20 of 356 found	Q8WXI7	Mucin-16	82.02	3.96	22	1518.2	5.26
	P15515	Histatin-1	68.85	36.84	2	7.0	9.13
	B7ZMD7	Alpha-amylase	66.23	29.16	8	57.7	6.93
	D3DPG0	Titin, isoform CRA_a	65.09	0.93	15	3878.8	6.38
	P02814	Submaxillary gland androgen-regulated protein 3B	61.25	65.82	2	8.2	9.57
	Q7Z5P9	Mucin-19	50.38	6.05	15	804.8	5.01
	B3KY63	cDNA FLJ16830 fis, clone UTERU3022536	43.22	4.77	5	215.1	5.90
	F5GZK2	Collagen alpha-1(XXI) chain	37.05	2.93	2	99.2	8.47
	P01036	Cystatin-S	33.12	32.62	3	16.2	5.02
	A0A0U1RR20	Proteoglycan 4	30.51	10.43	7	146.4	9.47
	Q86VQ1	Glucocorticoid-induced transcript 1 protein	29.92	15.54	4	58.0	9.44
	E9PAV3	Nascent polypeptide-associated complex subunit alpha, muscle-specific form	24.97	10.49	7	205.3	9.58
	Q5VST9	Obscurin	22.78	1.90	5	867.9	5.99
	H0Y465	Neurofibromin	20.65	2.88	2	281.0	7.28
	T1S9D5	MUC5AC	20.41	4.51	6	521.3	7.11
	T1R7N3	MUC5AC	20.12	7.13	6	413.6	8.09
	B4DH81	cDNA FLJ61250	19.95	4.74	2	93.5	6.92
	B3KY54	cDNA FLJ46886	19.84	5.48	2	61.6	7.75
	Q5SYE7	NHS-like protein 1	19.49	5.90	4	170.6	6.96
	Q9UQ35	Serine/arginine repetitive matrix protein 2	19.23	5.78	6	299.4	12.06

Table 5. The 20 more abundant proteins on metallic and ceramic brackets categorized by biological function related to dental caries

Function of proteins	BMQ		CBMQ	
	Description	Accession	Description	Accession
Antimicrobial	Mucin-16	Q8WXI7	Mucin-16	Q8WXI7
	Histatin-1	P15515	Cystatin-S	P01036
			Cystatin-SN	P01037
			Immunoglobulin heavy constant alpha 1	P01876
			Immunoglobulin kappa light chain	P0DOX7
			Polymeric immunoglobulin receptor	P01833
			Protein S100-A9	P06702
			Protein S100-A8	P05109
			Lactotransferrin	E7ER44
Lubrication	Mucin-16	Q8WXI7	Mucin-16	Q8WXI7
	Proteoglycan 4	Q92954		
Remineralization	Histatin-1	P15515	Protein S100-A9	P06702
			Protein S100-A8	P05109
early dental plaque formation			Alpha-amylase 1	P04745
Inflammatory response			Albumin	F6KPG5
			Protein S100-A9	P06702
			Protein S100-A8	P05109

Tissue formation/ protein-protein interaction	Keratin, type I cytoskeletal 10	P13645		
	Titin	A0A0A0MTS7	Carbonic anhydrase 6	P23280
	Keratin 1	H6VRF8	Zinc-alpha-2-glycoprotein	P25311
			Keratin 1	H6VRF8
	Keratin, type I cytoskeletal 9	P35527	Prolactin-inducible protein	P12273
	Keratin, type II cytoskeletal 2 epidermal	P35908	Alpha-enolase	P06733
	Serine/arginine repetitive matrix protein 1	M0R088		
	cDNA FLJ46178 fis, clone TESTI4003944	B3KXW2		
	Collagen alpha-1(XXI)	F5GZK2		
	cDNA FLJ54657, highly similar to Keratin, type II cytoskeletal 6A	B4DRU6	-	
	cDNA FLJ58286, highly similar to Actin, cytoplasmic 2	B4DVQ0	-	
	RNA-binding protein 34	A2A2V2	-	
	cDNA FLJ30689 fis, clone FCBBF2000566	B3KNX8		
Unknown Function			IGK@ protein	Q6PJF2
	Submaxillary gland androgen-regulated protein 3B	P02814	Zymogen granule protein 16 homolog B	A0A0C4DGN4
	Uncharacterized protein C15orf39	Q6ZRI6	Submaxillary gland androgen-regulated protein 3B	P02814
	cTAGE family member 2	Q96RT6		
	Unconventional myosin-XVB	A0A0J9YYJ7		
	Fibrous sheath-interacting protein 2	Q5CZC0		

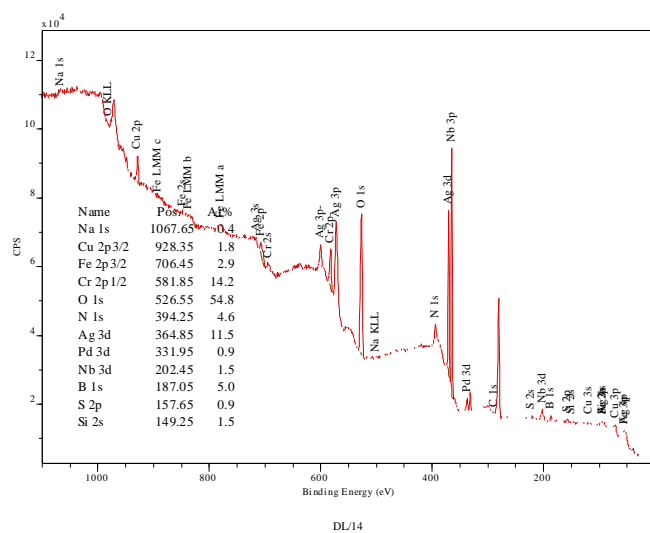| Name	Pos.	At%
Na 1s	1067.65	0.4
Cu 2p3/2	928.35	1.8
Fe 2p3/2	706.45	2.9
Cr 2p1/2	581.85	14.2
O 1s	526.55	54.8
N 1s	394.25	4.6
Ag 3d	364.85	11.5
Pd 3d	331.95	0.9
Nb 3d	202.45	1.5
B 1s	187.05	5.0
S 2p	157.65	0.9
Si 2s	149.25	1.5

DL/14

Figure 1. XPS wide scan spectrum of metallic brackets surface pre-treated with distilled water

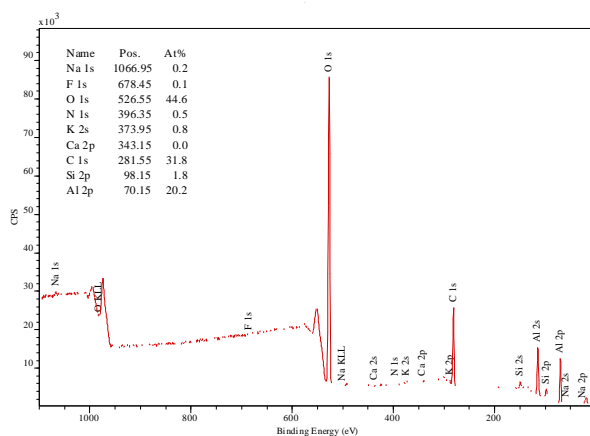| Name	Pos.	At%
Na 1s	1066.95	0.2
F 1s	678.45	0.1
O 1s	526.55	44.6
N 1s	396.35	0.5
K 2s	373.95	0.8
Ca 2p	343.15	0.0
C 1s	281.55	31.8
Si 2p	98.15	1.8
Al 2p	70.15	20.2

Figure 2. XPS wide scan spectrum of ceramic orthodontic brackets surfaces pre-treated with distilled water

Figure 3. Venn diagram of acquired pellicle proteins identified in each material surface group and across groups. BMQ: metallic orthodontic bracket, CBMQ: Ceramic orthodontic bracket, DMQ: HA discs
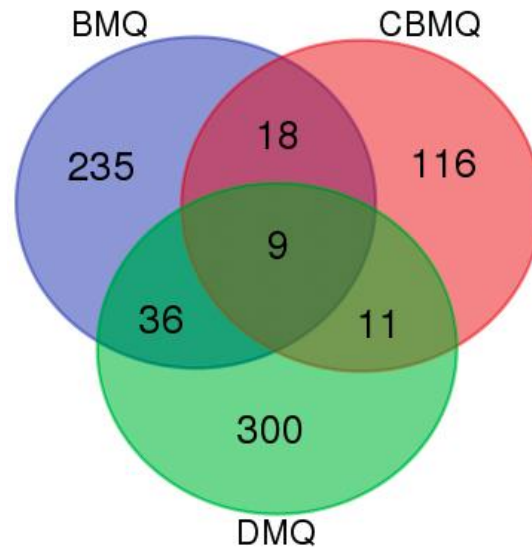
Appendix 1: BCA of pooled saliva prior any incubation treatment

	Standards								
Ave	2.1995	1.7655	1.291	1.061	0.7455	0.4555	0.2585	0.118	0.0835
Ave corr	2.116	1.682	1.2075	0.9775	0.662	0.372	0.175	0.0345	0
[] ug/ml	2000	1500	1000	750	500	250	125	25	0

	Water	WSS pool	wash-1	elution-1	f.1x-2	wash-2	elution-2	f.1x-3	wash-3	elution-3
Ave	0.085	1.251								
Ave corr	0.0015	1.1675								
[] ug/ml	- 65.45454545	994.5454545								
800ug	- 12222.22222	804.3875686								
20ug	- 305.5555556	20.10968921								
25ug	381.9444444	25.13711152								

$y = 0.0011x + 0.0735$
$R^2 = 0.9915$
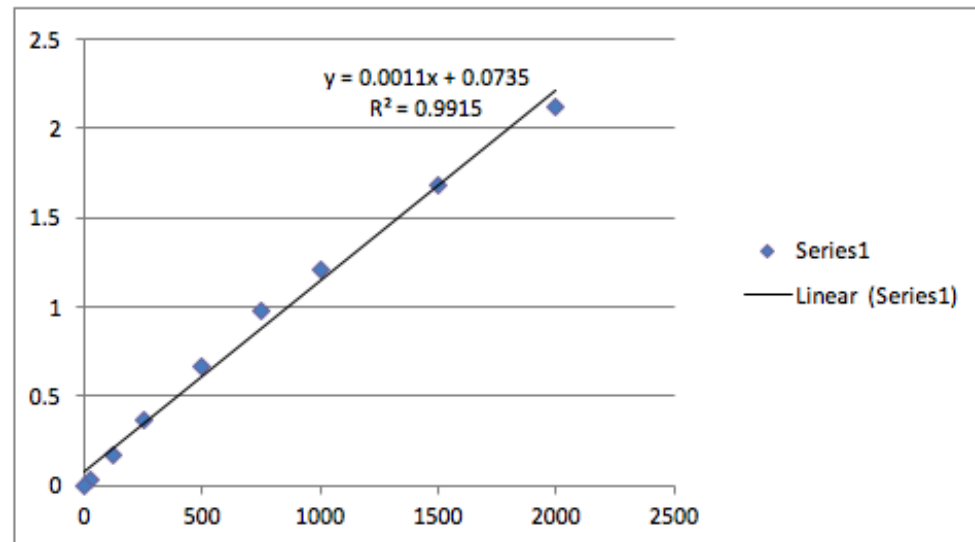
Appendix 2: µBCA of observed Acquired Pellicle on HA discs and orthodontic brackets after incubation with whole saliva supernatant

	2.533	0.904	0.533	0.27	0.134	0.087	0.094	0.052	0.058
	2.572	0.925	0.468	0.253	0.126	0.083	0.063	0.063	0.07
Ave	2.5525	0.9145	0.5005	0.2615	0.13	0.085	0.0785	0.0575	0.064
Ave corr	2.4885	0.8505	0.4365	0.1975	0.066	0.021	0.0145	-0.0065	0
[ ] ug/ml	200	40	20	10	5	2.5	1	0.5	0
y acc equation	2.6058	0.9258	0.4638	0.2118	0.08055	0.0136125	-0.02697	0.0405675	-0.0542
diference	0.1173	0.0753	0.0273	0.0143	0.01455	0.0073875	-0.04147	0.0340675	-0.0542

$y = -6E-05x^2 + 0.024x - 0.0243$
$R^2 = 0.99961$
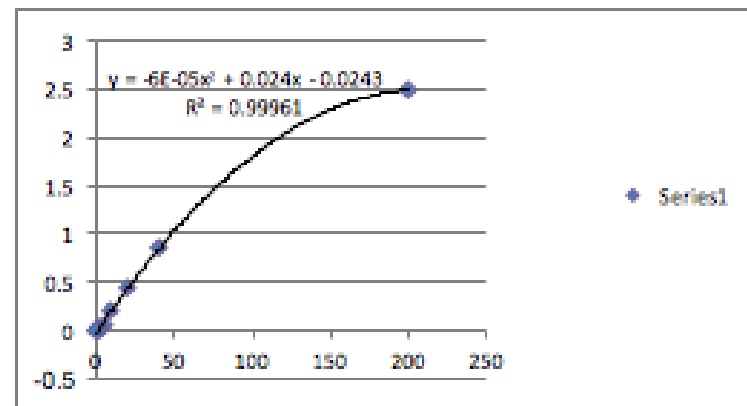
Samples	DL	DW	DNaF	BL	BW	BNaF
[ ] ug/ml	40.67	39.91	28.0	31.80	31.32	26.28
15 µg	369	376	538	472	479	571

Appendix 3: Material safety data sheet from Orthodontic company

MATERIAL SAFETY DATA SHEET   Page 1 of 2
MSDS Palladium Braze.doc

SECTION I – PRODUCT AND COMPANY IDENTIFICATION	
Company Name	Emergency telephone number
American Orthodontics	**(920) 457-5051**
3524 Washington Ave	Telephone for information
Sheboygan Wisconsin 53081	**(920) 457-5051**

Product Identification:

Product Name	Palladium Brazing Alloy
Common Name	Brazing Compounds
Associated Catalog Numbers	Various products brazed or soldered during manufacture

SECTION II – HAZARDOUS COMPONENTS				
Ingredients Considered Hazardous	Common Name	CAS Number	OSHA PEL	ACGIH TLV
	Copper, Cu	7440-50-8	1.0	1.0
	Nickel, Ni	7440-02-0	1.0	1.0
	Palladium, Pd	7440-05-3	N/E	N/E
	Silver, Ag	7440-22-4	0.01	0.1

N/E = None Established

Western
Research

Western University Health Science Research Ethics Board
HSREB Annual Continuing Ethics Approval Notice

Date: June 06, 2016
Principal Investigator: Dr. Walter Siqueira
Department & Institution: Schulich School of Medicine and Dentistry\Dentistry,Western University

Review Type: Expedited
HSREB File Number: 6251
Study Title: Composition, Structure and Function of Salivary Proteins
Sponsor: Natural Sciences and Engineering Research Council

HSREB Renewal Due Date & HSREB Expiry Date:
Renewal Due -2017/05/31
Expiry Date -2017/06/25

The Western University Health Science Research Ethics Board (HSREB) has reviewed the Continuing Ethics Review (CER) Form and is re-issuing approval for the above noted study.

The Western University HSREB operates in compliance with the Tri-Council Policy Statement Ethical Conduct for Research Involving Humans (TCPS2), the International Conference on Harmonization of Technical Requirements for Registration of Pharmaceuticals for Human Use Guideline for Good Clinical Practice (ICH E6 R1), the Ontario Freedom of Information and Protection of Privacy Act (FIPPA, 1990), the Ontario Personal Health Information Protection Act (PHIPA, 2004), Part 4 of the Natural Health Product Regulations, Health Canada Medical Device Regulations and Part C, Division 5, of the Food and Drug Regulations of Health Canada.

Members of the HSREB who are named as Investigators in research studies do not participate in discussions related to, nor vote on such studies when they are presented to the REB.

The HSREB is registered with the U.S. Department of Health & Human Services under the IRB registration number IRB 00000940.

CURRICULUM VITAE

Maria Pia Canales, DMD

Languages: Fluent in French, English and Spanish

EDUCATION

2015 – 2018 **WESTERN UNIVERSITY**	Master of Clinical Dentistry (MCID)
2012-2013 *BOSTON UNIVERSITY*	Certificate in Advanced General Studies (AEGD)
2007 - 2012 *UNIVERSITÉ DE MONTRÉAL*	*DMD – Doctor of Dental Medicine* - *Honors received by ''ADQPPA''*
2004 - 2006 *COLLÈGE JEAN-DE-BRÉBEUF*	D.E.C. – College Degree in Natural Science
1999 - 2004 *COLLÈGE DUROCHER ST-LAMBERT*	D.E.S. High School Diploma

PROFESSIONAL EXPERIENCE

2013 – 2015 *CLINIQUE RUE ROY*	General Dentist
May 2012 *UNIVERSITÉ DE MONTRÉAL*	Oral and maxillofacial surgery assistant Continuing dental education
2004 – 2006 *COLLEGE JEAN-DE-BRÉBEUF*	Mathematics and physics tutor

ACTIVITIES

2013 – 2015 *DENTISTE SANS FRONTIÈRE*	**Active Member** -Fundraising and providing dental care in developing countries

2004-2006
AMNESTY INTERNATIONAL   **Active Member**
-Campaigning for human rights

2004 à 2006
SAINTE-JUSTINE HOSPITAL   **Volunteer**
-Help parents move to Ronald McDonald residence
-Provide moral support to the parents of the patients

PERSONNEL INTEREST

Volley-ball, yoga, running, cycling and cooking